

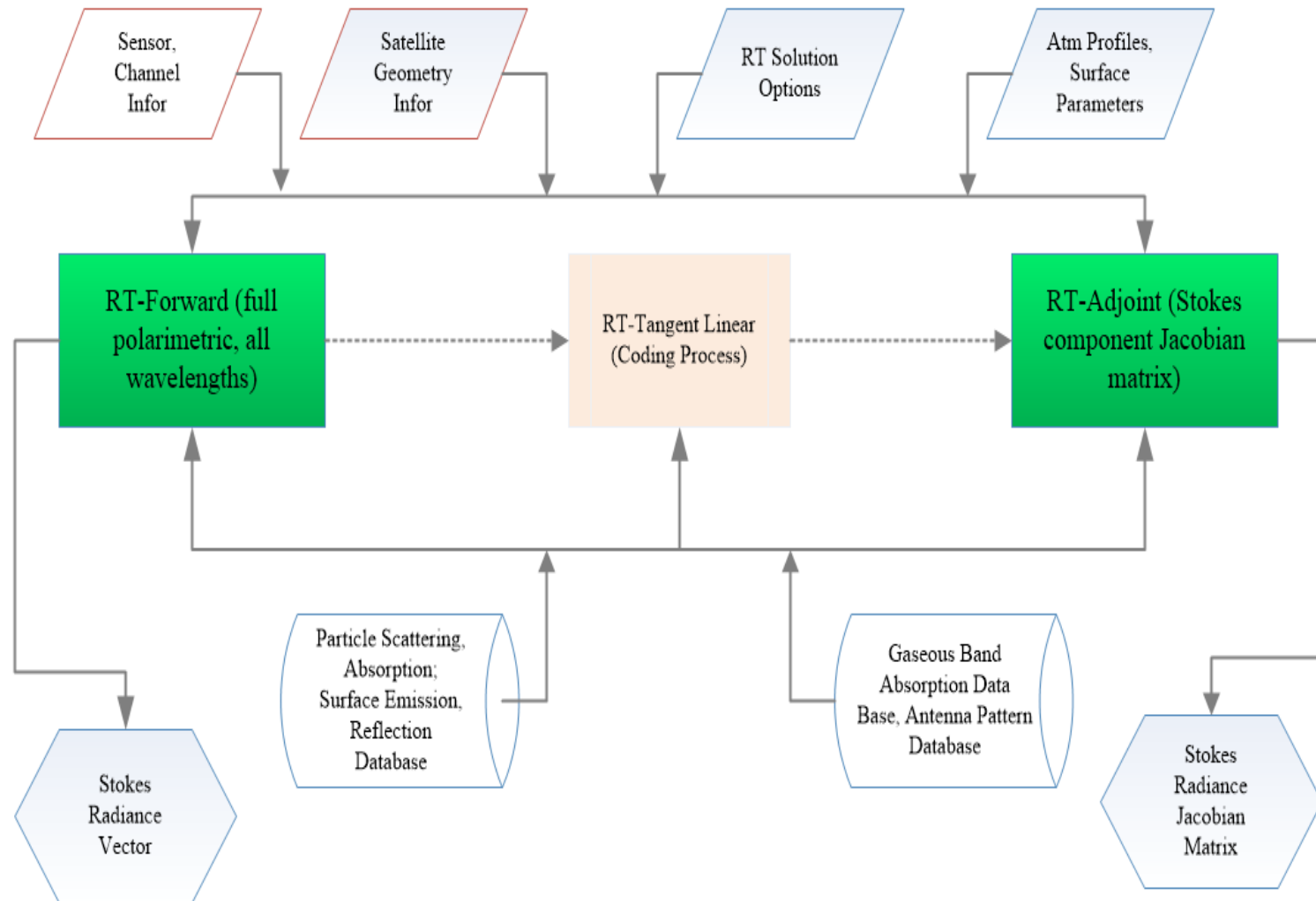
# **Simulations and Observations of Surface Properties for Supporting Satellite Data Assimilation**

Fuzhong Weng

State Key Laboratory of Severe Weather, Beijing, China

*2019 International Workshop of Radiative Transfer Model for Satellite Data  
Assimilation, Tianjin, China, 4/29-5,3, 2019*

# Advanced Radiative Transfer Modeling System (ARMS)



# ARMS Uniqueness

- Improve the performance of simulated radiance under aerosols, cloudy and precipitation conditions through better scattering tables
- Improve the accuracy in simulating TOA radiances through vector radiative transfer models
- Adapt the analytic adjoint models developed earlier for vector matrix operator, DISORT and VDISORT
- Increase the computational speeds in scattering conditions through GPU and better software engineering
- Prepare NWP community full readiness for using a variety of Chinese instruments (e.g. FY, HY and GF)
- Improve surface emissivity modeling over Chinese western parts (e.g. Plateau) and polar regions, aka three poles

# Surface Emissivity Models

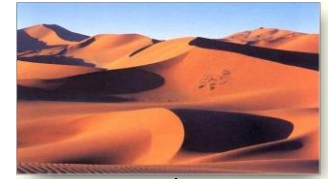
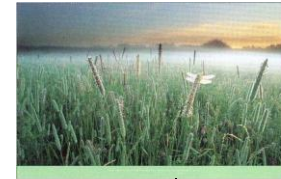
Ocean

Sea Ice

Snow

Canopy (bare soil)

Desert



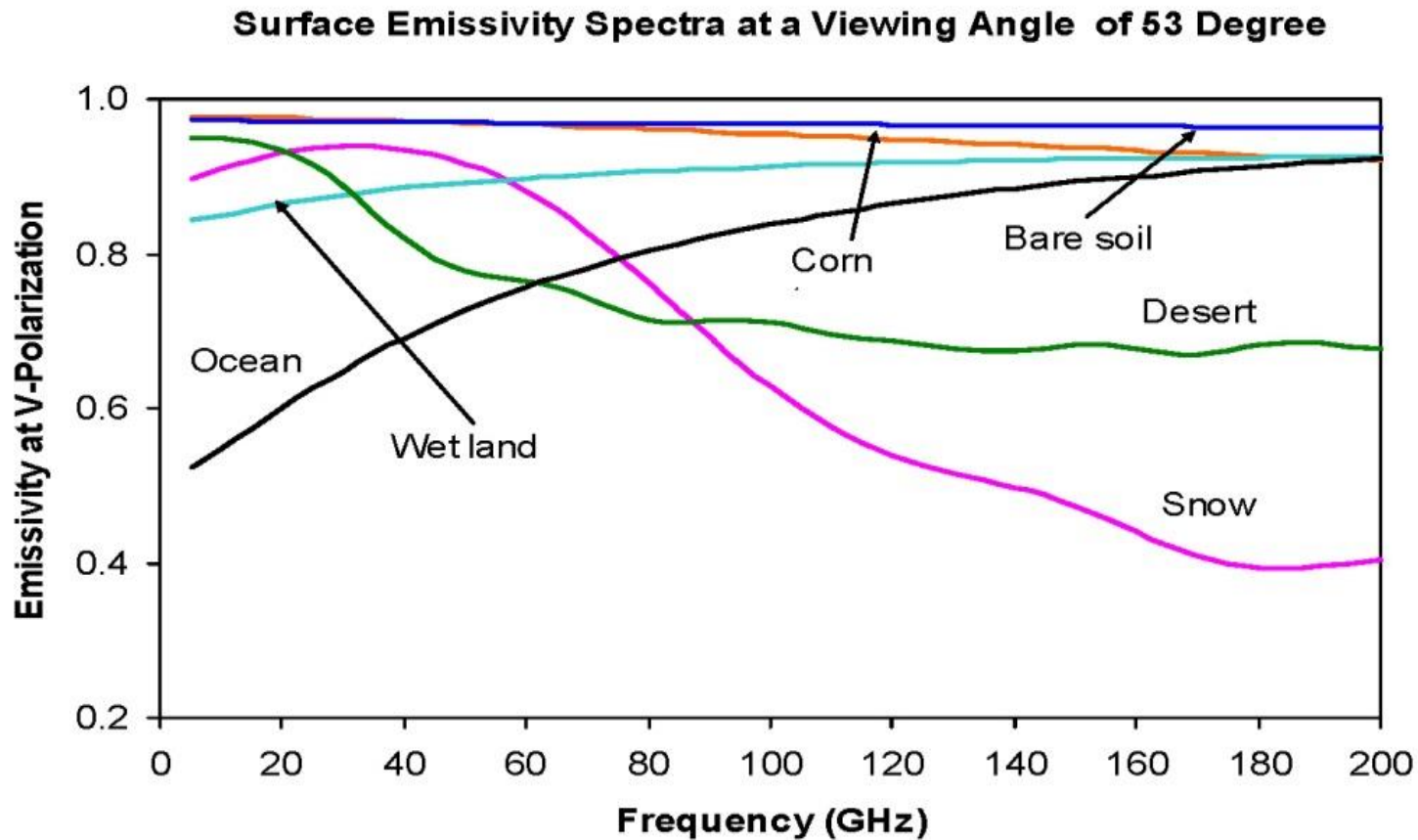
Microwave land emissivity model (NESDIS model) (Weng et al, Yan, Grody, 2001), desert microwave emissivity library (Yan and Weng, 2011) TELSEM, and CNRM databases (Prigent, 200x)  
Vegetation (Chen and Weng, 2014)  
Surface roughness (Chen and Weng, 2015)

NPOESS Infrared emissivity database  
IASI Land Infrared emissivity database  
UWIREMIS database

Empirical snow and sea ice microwave emissivity algorithm (Yan and Weng, 2003; 2008)

FASTEM microwave emissivity model (Liu et al., 2010, English, 199x)  
IR emissivity model (Wu and Smith, 1991; van Delst et al., 2001; Nalli et al., 2008)

# Microwave Emissivity Spectra over Various Surface Conditions



# Refractivity or Emissivity for a Flat Surface

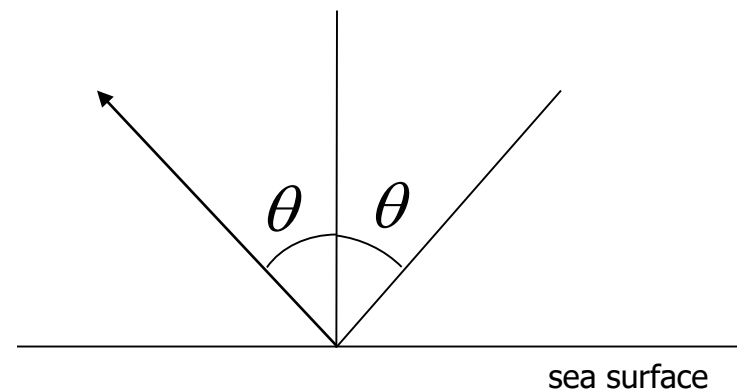
$$\varepsilon_p(\nu, \theta) = 1 - \Gamma_p(\nu, \theta) \quad (p = h \text{ or } v)$$

$\Gamma_p(\nu, \theta)$  Total Reflectivity    $\nu$  Frequency    $\theta$  Zenith angle

For a specular surface, reflectivity can be calculated by Fresnel law:

$$\Gamma_v = \frac{\varepsilon_v(\nu, \theta) \cos \theta - \sqrt{\varepsilon_v(\nu, \theta) - \sin^2 \theta}}{\varepsilon_v(\nu, \theta) \cos \theta + \sqrt{\varepsilon_v(\nu, \theta) - \sin^2 \theta}}$$

$$\Gamma_h = \frac{\cos \theta - \sqrt{\varepsilon_h(\nu, \theta) - \sin^2 \theta}}{\cos \theta + \sqrt{\varepsilon_h(\nu, \theta) - \sin^2 \theta}}$$



# Foam Coverage Formula

Foam is a mixture of air and water and has a higher emissivity than flat water

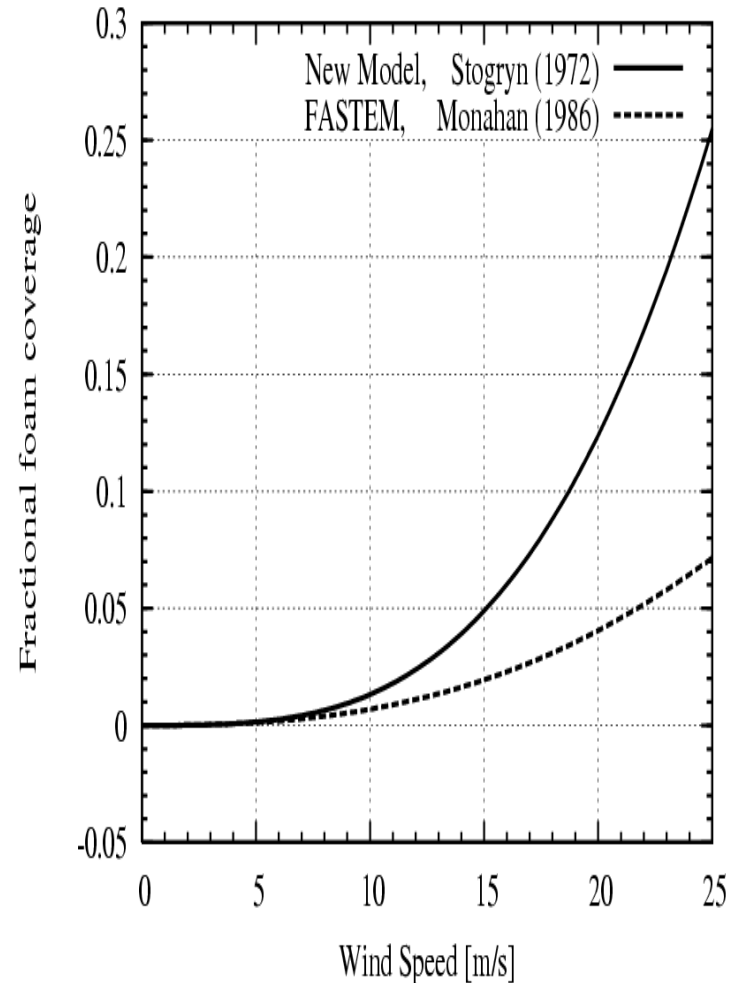
Foam coverage:

Stogryn, 1972

$$f_c = 7.75 \times 10^{-6} \left( \frac{V}{V_0} \right)^{3.231}$$

Monahan, 1986

$$f = 1.95 \times 10^{-5} u^{2.55}$$



# Foam Emissivity vs. Angle

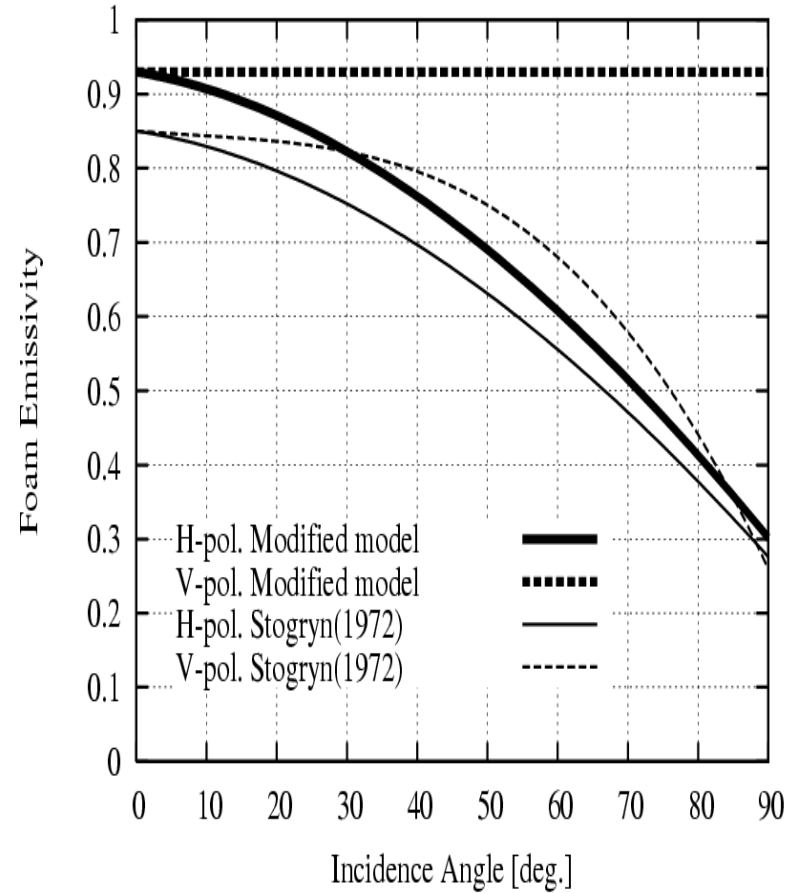
Foam emissivity (angular dependent and frequency dependent):

H-Pol

$$r_{\text{foam}} = 1.0 - (208.0 + 1.29e-9 * f) / t * g$$

V-Pol

$$r_{\text{foam}} = 1.0 - (208.0 + 1.29e-9 * f) / t * g$$





# Total Reflectivity (1 - Emissivity)

$$\Gamma_p(\nu, \theta, T_s, W, S) = f(\nu, \theta, W) \left| R_{p, \text{Foam-covered}}(\nu, \theta, T_s, W) \right|^2 \\ + (1 - f(\nu, \theta, W)) \left| R_{p, \text{Foam-free}}(\nu, \theta, T_s, W, S) \right|^2$$

where

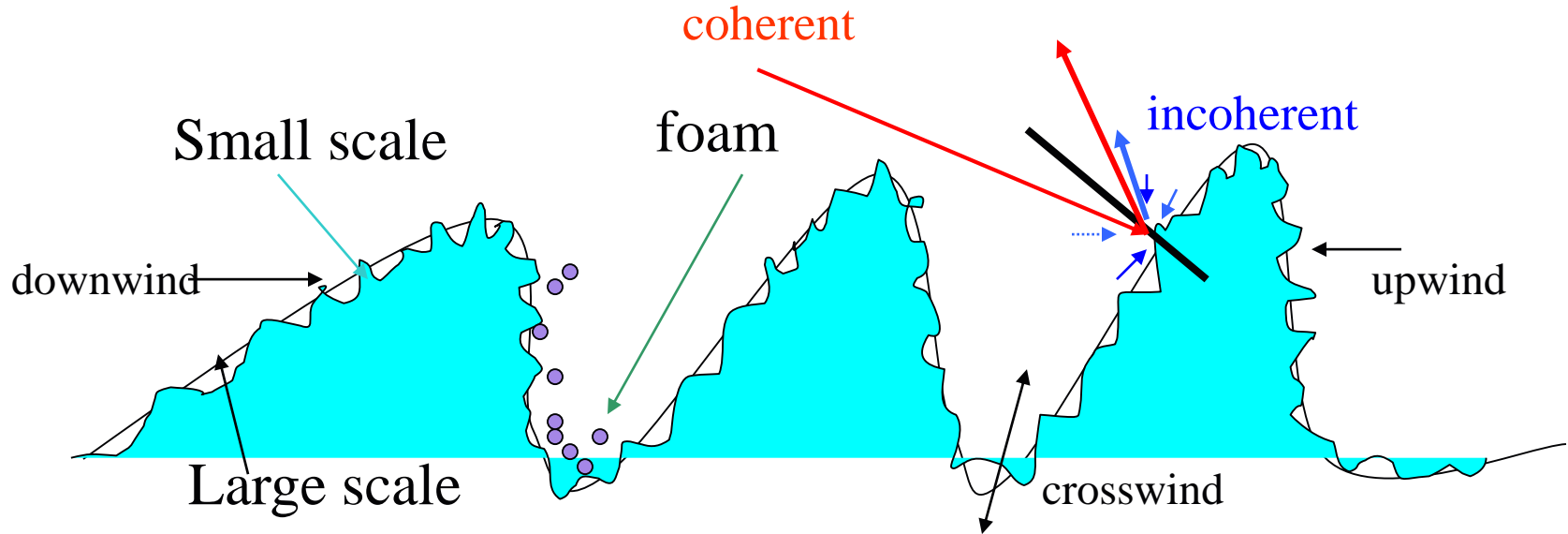
W: Wind speed

$\theta$ : local zenith angle

S: Salinity

Ts: sea surface temperature

# Ocean Roughness and Emissivity Model



The large-scale roughness is dependent on the gravity waves and whereas the small irregularities is affected by capillary waves. There are coherent reflection and incoherent scattering associated with the waves in both scales

# Stokes Vector Reflectivity or Emissivity

$$\mathbf{A} = \mathbf{A}_{co} + \mathbf{A}_{in}$$

Coherent term is related to the reflection of large scale roughness):

$$\mathbf{A}_{co} = \frac{4\pi\delta(\mu - \mu')\delta(2\pi + \phi - \phi')}{(1 - \mu^2)^{\frac{1}{2}}} \times \begin{pmatrix} |R_{ll}|^2 & |R_{lr}|^2 & Re(R_{rr}R_{rl}^*) & -Im(R_{rr}R_{rl}^*) \\ |R_{rl}|^2 & |R_{rr}|^2 & Re(R_{lr}R_{ll}^*) & -Im(R_{lr}R_{ll}^*) \\ 2Re(R_{rl}R_{ll}^*) & 2Re(R_{rr}R_{lr}^*) & Re(R_{rr}R_{ll}^* + R_{rl}R_{lr}^*) & -Im(R_{rr}R_{ll}^* - R_{rl}R_{lr}^*) \\ 2Im(R_{rl}R_{ll}^*) & 2Im(R_{rr}R_{lr}^*) & Im(R_{rr}R_{ll}^* + R_{rl}R_{lr}^*) & Re(R_{rr}R_{ll}^* - R_{rl}R_{lr}^*) \end{pmatrix}$$

$$\mathbf{R} = \begin{pmatrix} R_{ll}^{(0)} + R_{ll}^{(2)} & R_{lr}^{(2)} \\ R_{rl}^{(2)} & R_{rr}^{(0)} + R_{rr}^{(2)} \end{pmatrix},$$

$$R_{\alpha\beta}^{(2)}(\theta, \phi) = \int_0^{2\pi} \int_0^\infty k_0^2 W_s(k_{\rho i} \cos\phi - k_\rho \cos\phi', k_{\rho i} \sin\phi - k_\rho \sin\phi') g_{\alpha\beta}^{(2)} k_\rho d\phi',$$

# Stokes Vector Reflectivity or Emissivity

Incoherent term is related to the reflection of small scale roughness:

$$\mathbf{A}_{in} = \begin{pmatrix} \gamma_{lll} & \gamma_{lrl} & \text{Re}(\gamma_{rrl}) & \text{Im}(\gamma_{rrl}) \\ \gamma_{rlr} & \gamma_{rrr} & \text{Re}(\gamma_{lrl}) & \text{Im}(\gamma_{lrl}) \\ 2\text{Re}(\gamma_{rll}) & 2\text{Re}(\gamma_{rrl}) & \text{Re}(\gamma_{rll} + \gamma_{rll}) & -\text{Im}(\gamma_{rll} - \gamma_{rll}) \\ 2\text{Im}(\gamma_{rll}) & 2\text{Im}(\gamma_{rrl}) & \text{Im}(\gamma_{rll} + \gamma_{rll}) & \text{Re}(\gamma_{rll} - \gamma_{rll}) \end{pmatrix},$$

$$\gamma_{pq\alpha\beta}(\theta, \phi, \theta', \phi') = 4\pi k_0^4 \cos\theta' F_{pq\alpha\beta}(\theta, \phi, \theta', \phi')$$

# Stokes Vector Emissivity Wave Spectrum Function ( $W_s$ )

$$W(K, \varphi) = \frac{1}{2\pi K} S(K) \Phi(K, \varphi)$$

$S(K)$  is an omni-directional spectrum

$\Phi(K, \varphi)$  is the angular portion of the spectrum

$\varphi$  is the wave direction relative to wind

$$\Phi(K, \varphi) = 1 + d[1 - \exp(-sK^2)] \cos 2\varphi$$

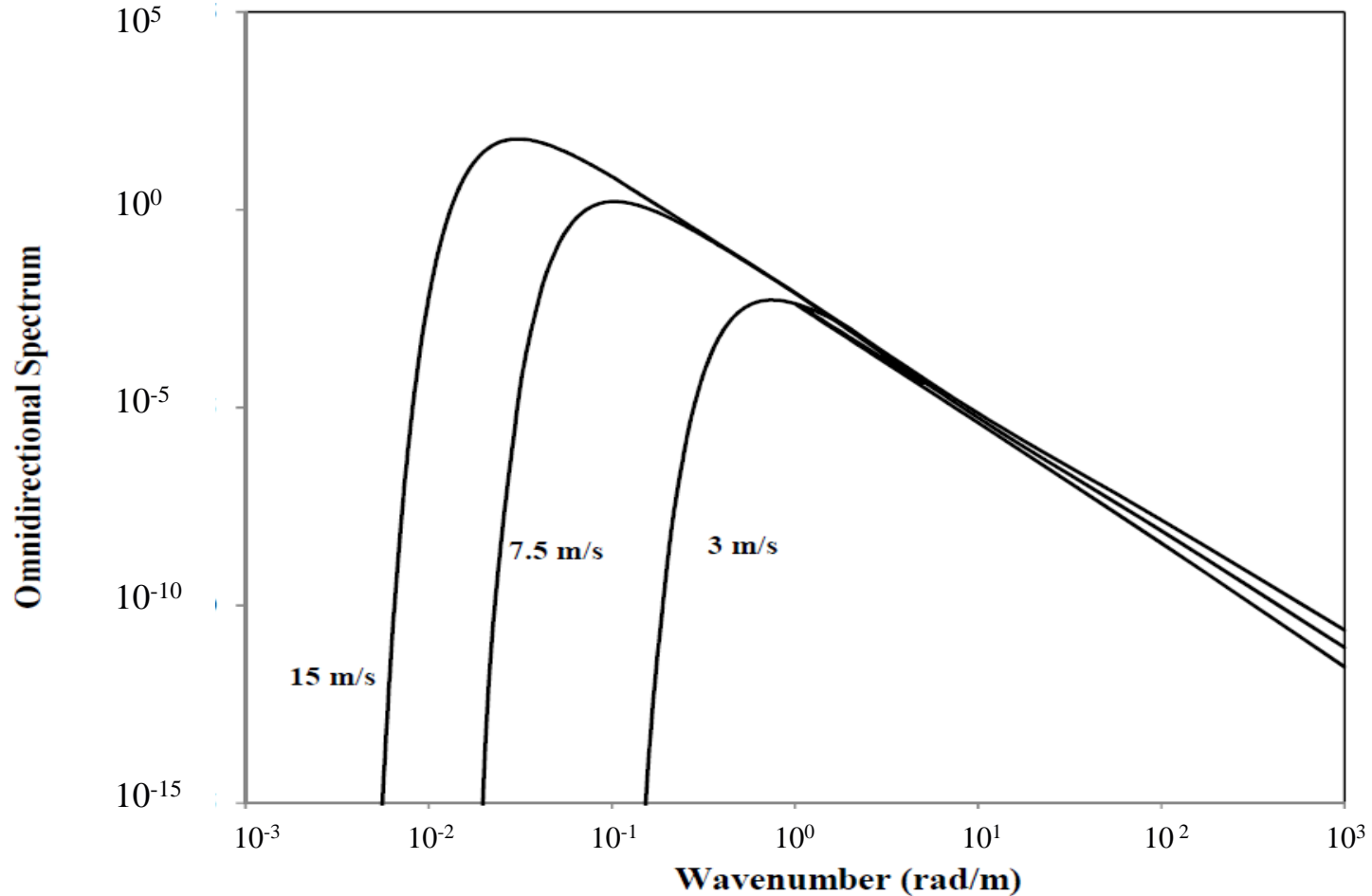
when  $K < K_j$

$$S(k) = \frac{a}{2\pi} K^{-3} \exp[-0.74(K_0 / K)^2]$$

When  $K \geq K_j$

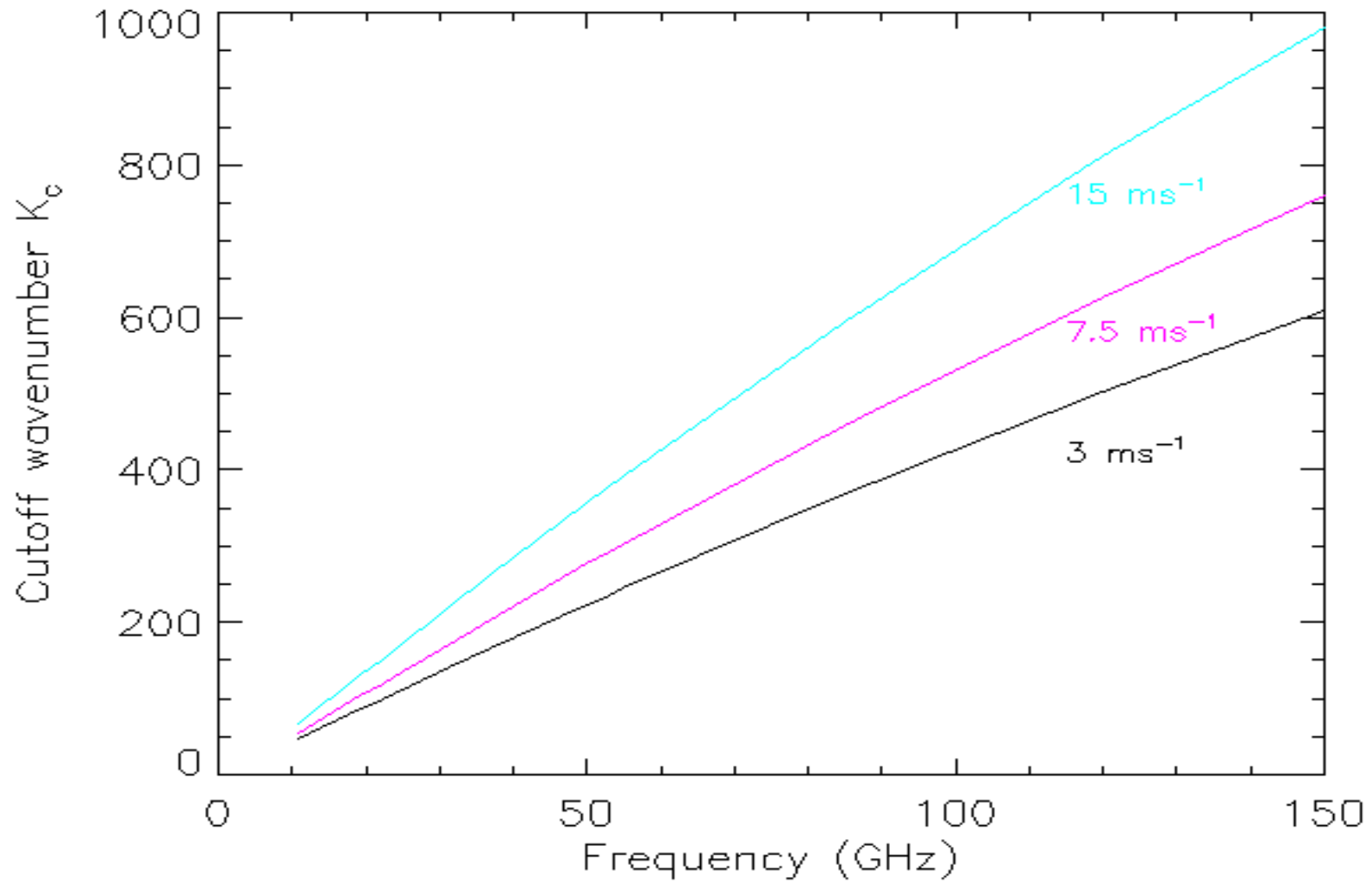
$$S(K) = \frac{a}{2\pi} K^{-3} \left( \frac{bKu_*^2}{g + \gamma K^2} \right)^{c \log_{10}(K / K_j)} \exp[-0.74(K_0 / K_j)^2]$$

# Bjerkaas/Riedel (BR) Ocean Roughness Spectrum



(Elfouhaily et al., 1997).

# Cutoff Wavenumber



# Water Permittivity Models

- Permittivity models are either single or double Debye's formula, taking into account polarization.
  - Single Debye's model: Stogryn, 1971; Klein and Swift, 1977; Ellison et al., 1998; Guillou et al., 1998.
  - Double Debye's model: Ellison et al., 2003; Meissner and Wentz, 2004; Romaraju and Trumpf, 2006.
- For a low frequency ( $< 20$  GHz), permittivity depends on salinity
- Permittivity model of Ellison et al. (2003) is used in the FASTEM emissivity model



# Ocean Permittivity Model (1/2)

Debye (1929) model for pure water, the permittivity

$$\epsilon = \epsilon_{\infty} + \frac{\epsilon_s - \epsilon_{\infty}}{1 + j2\pi f\tau}$$

Dissolved salt in water will be a good conductor and contributes to imaginary part

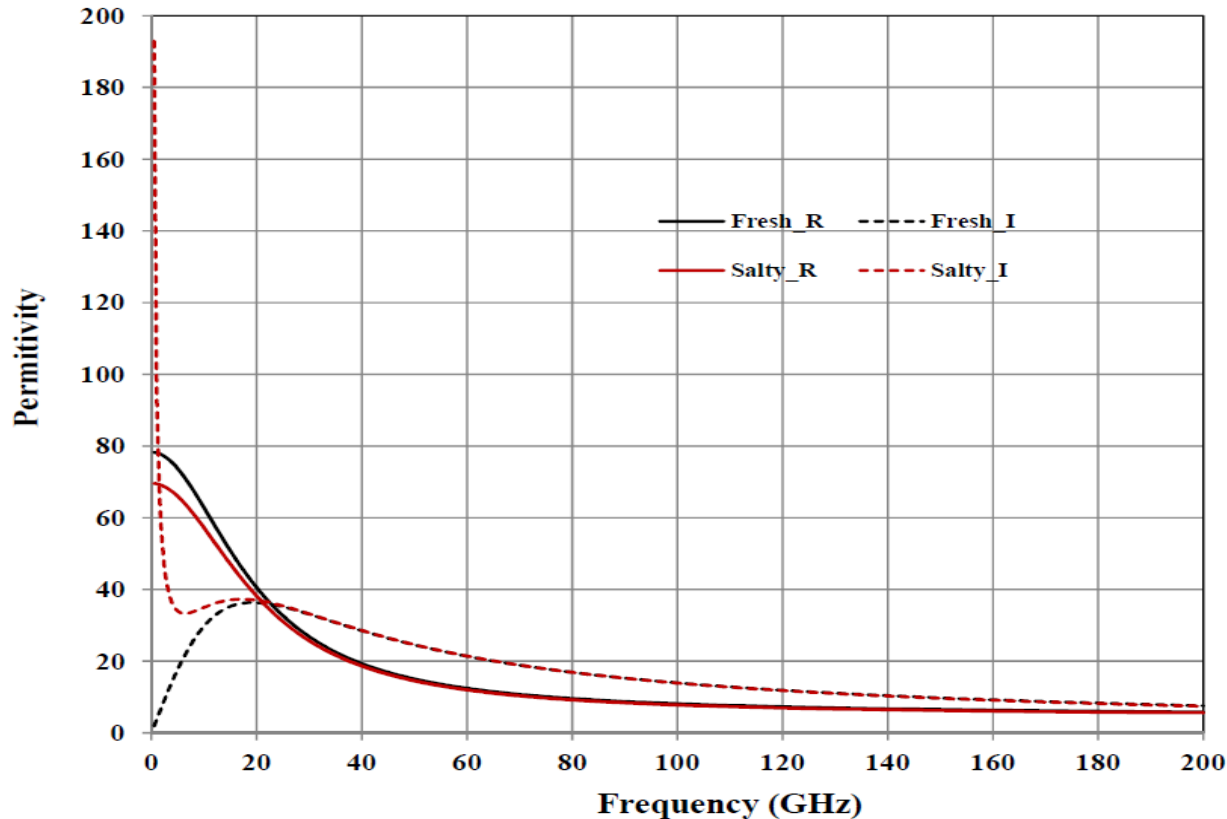
$$\epsilon = \epsilon_{\infty} + \frac{\epsilon_s - \epsilon_{\infty}}{1 + j2\pi f\tau} + j \frac{\alpha}{2\pi f\epsilon_0}$$

For a better performance at higher frequency, it is found that double Debye is needed with

$$\epsilon = \epsilon_{\infty} + \frac{\epsilon_s - \epsilon_1}{1 + j2\pi f\tau_1} + \frac{\epsilon_1 - \epsilon_{\infty}}{1 + j2\pi f\tau_2} + j \frac{\alpha}{2\pi f\epsilon_0}$$

$\epsilon_1$  is the permittivity at an intermediate frequency

# Water Permittivity vs. Frequency

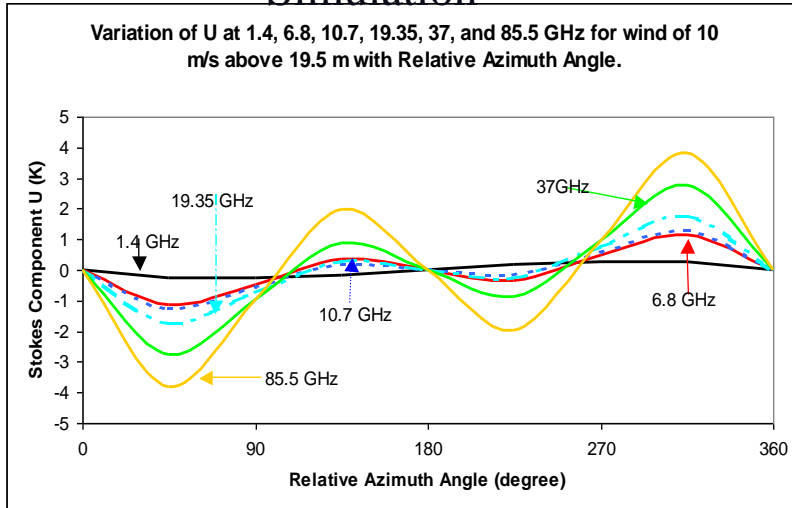


The permittivity model of Ellison (2003) is for a fixed salinity of 35%. The permittivity model of Somaraju and Trumpf (2006) has a simple expression, but its empirical coefficients were not derived from measurements. The model of Meissner and Wentz (2004) can be used for frequencies up to 500 GHz. The model fits measurements well. But its permittivity at an infinitive frequency depends on salinity, conflict with physics. Our model removes the salinity dependency and revises fitting coefficients

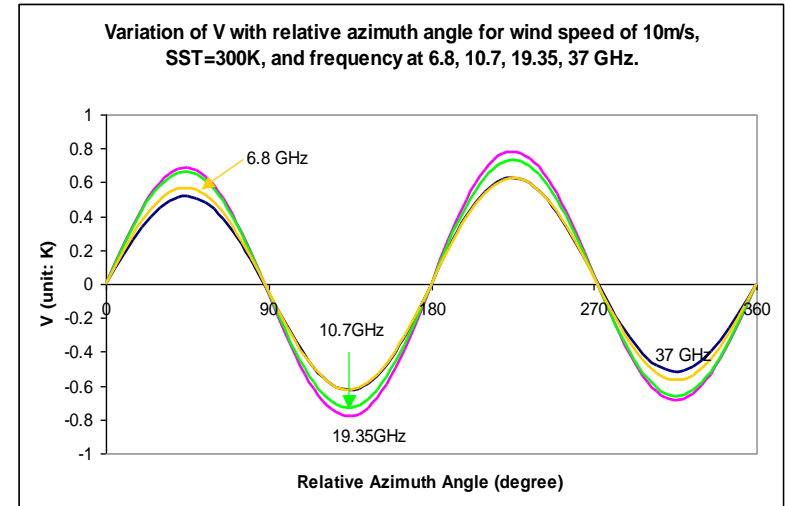
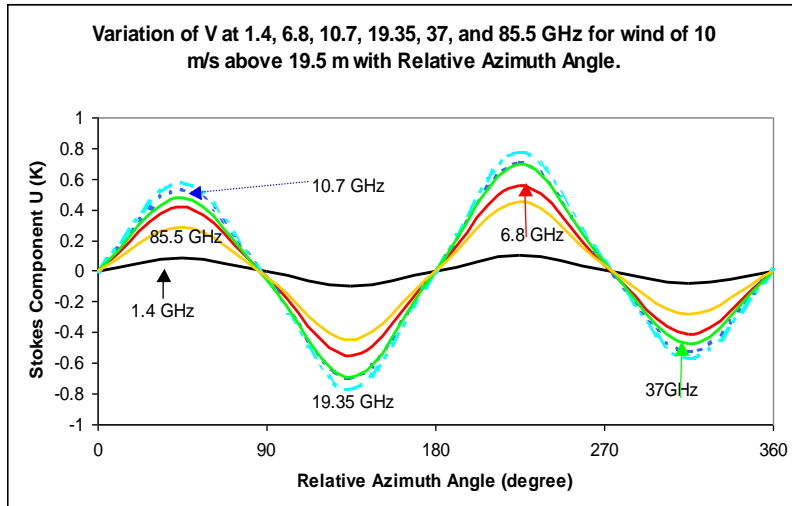
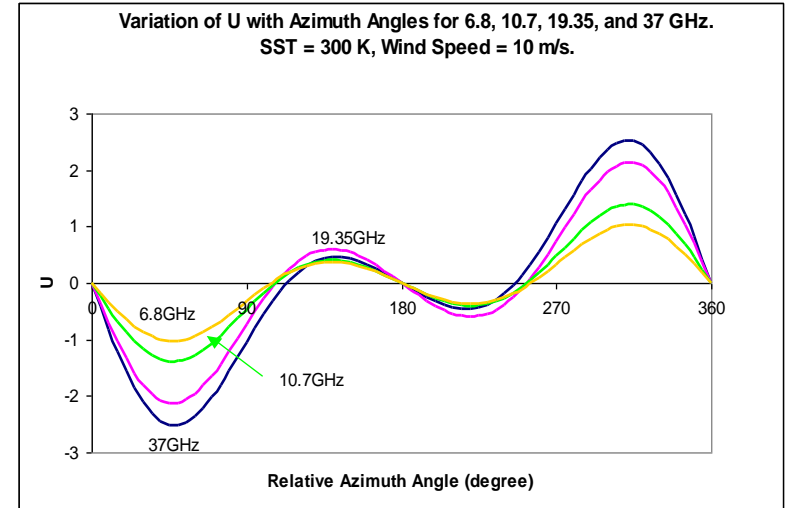
Black line for fresh water and red line for sea water. The symbol squares are measurements for fresh water (black) and sea water (red).

# Oceanic Emission Model vs. Observations

## Simulation

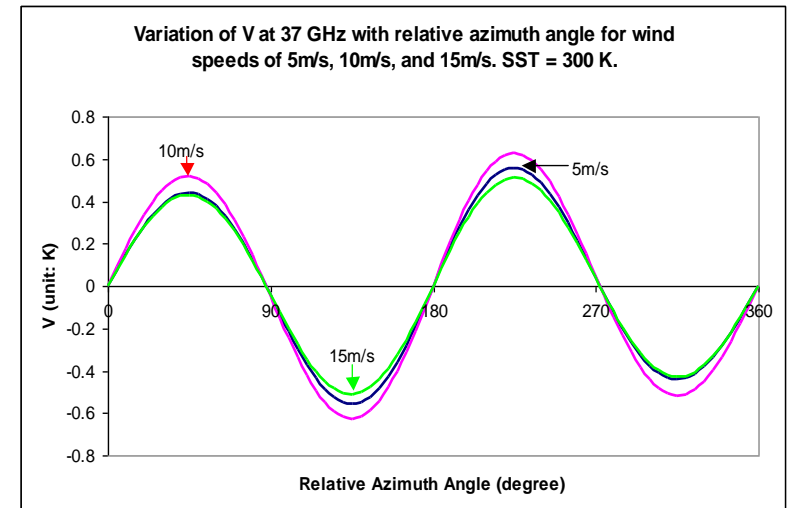
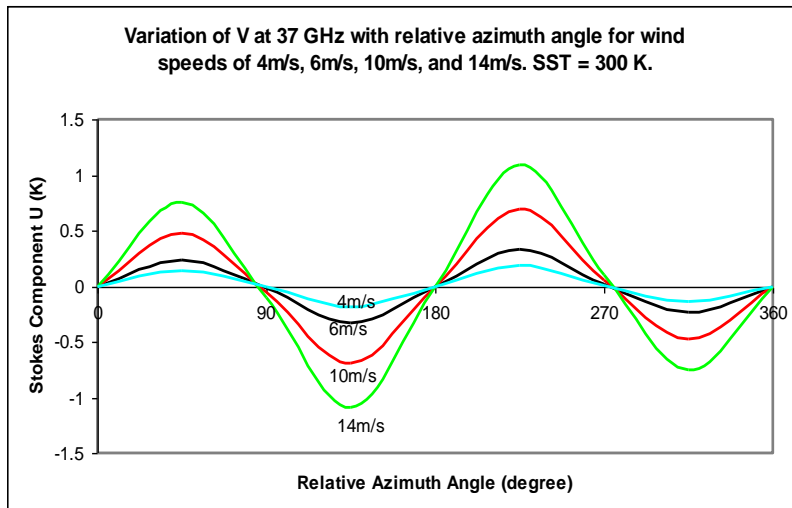
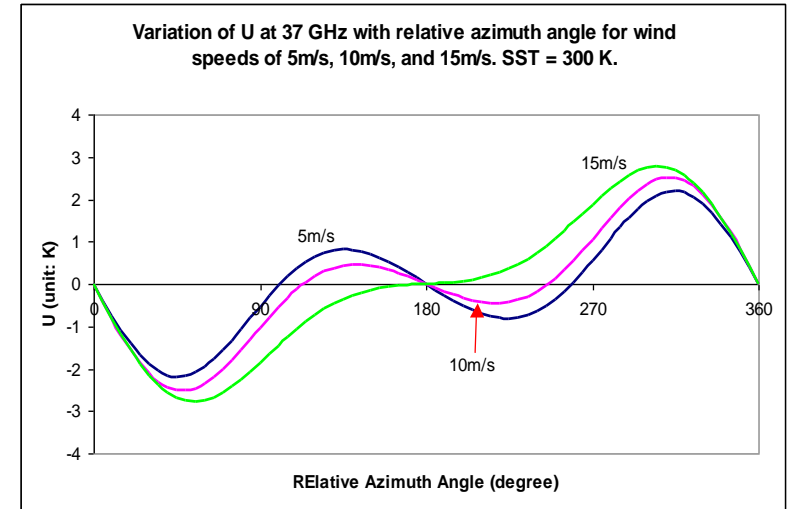
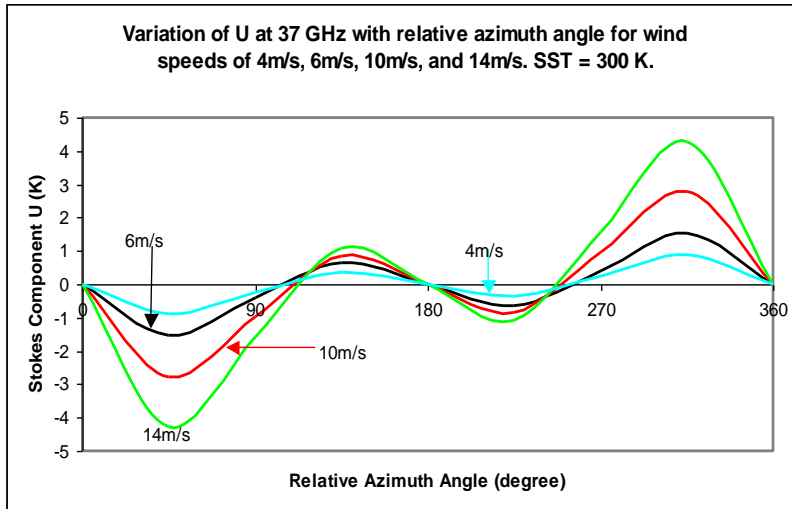


## Measurement



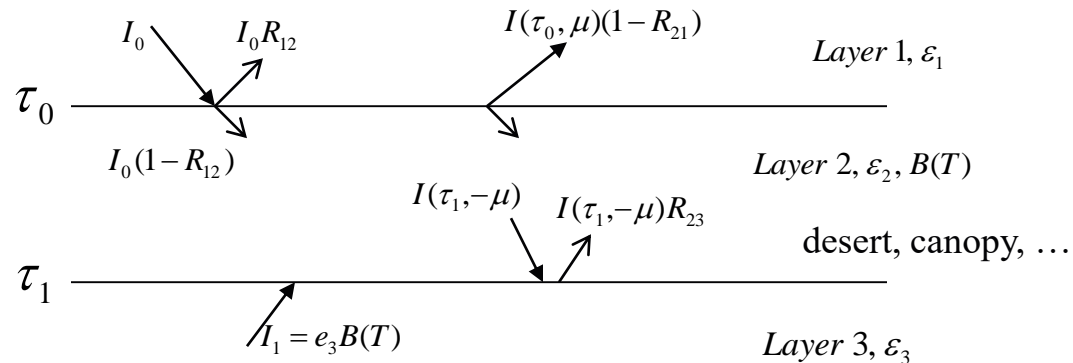
# Oceanic Emission Model vs. Observations

## Simulation



# Microwave Land Emissivity Model (LandEM)

(1) Three layer medium:



(2) Emissivity derived from a two-stream radiative transfer solution and modified Fresnel equations for reflection and transmission at layer interfaces:

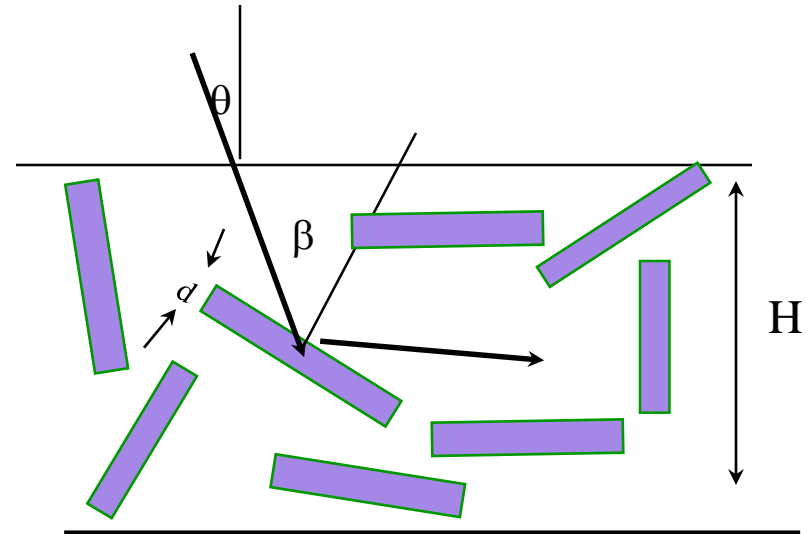
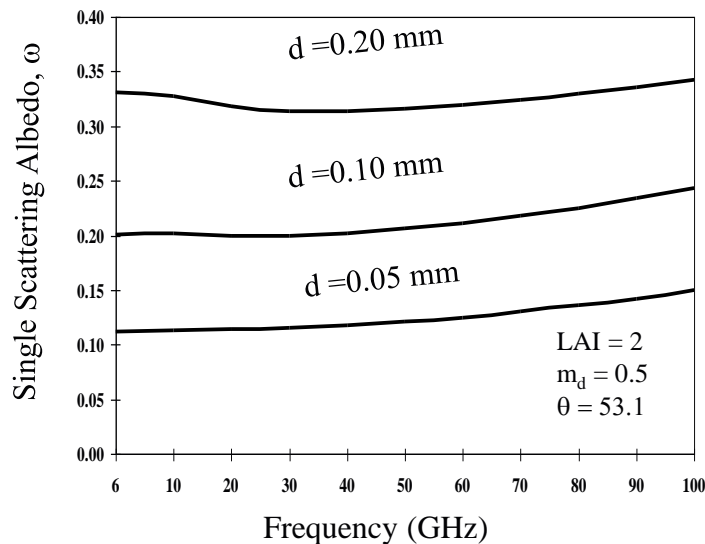
$$e = \alpha R_{12} + (1 - R_{21}) \frac{(1 - \beta)[1 + \gamma e^{-2k(\tau_1 - \tau_0)}] + \alpha(1 - R_{12})[\beta - \gamma e^{-2k(\tau_1 - \tau_0)}]}{(1 - \beta R_{21}) - (\beta - R_{21})\gamma e^{-2k(\tau_1 - \tau_0)}}$$

Weng, et al, 2001

# Optical Properties for Vegetation Canopy

Geometric optics is applied because the leaf size is typically larger than wavelength

- Wegmuller et al.'s derivation
- Canopy leaves are oriented
- Matzler's dielectric constant



$d$  - leaf thickness

$H$  - canopy height

LAI - leaf area index

$m_d = \text{dry matter content} = 0.84m_d + 0.51$

$\beta$  - leaf orientation angle

$\theta$  - incident angle of EM wave

# Land Surface Roughness Model

$$R_p = [(1 - Q)r_p + Qr_q]P$$

Wang's model ( $h = 4k^2\sigma^2$ ): L-band

$$P(k, \sigma, \vartheta) = \exp(-4k^2\sigma^2 G(\vartheta))$$

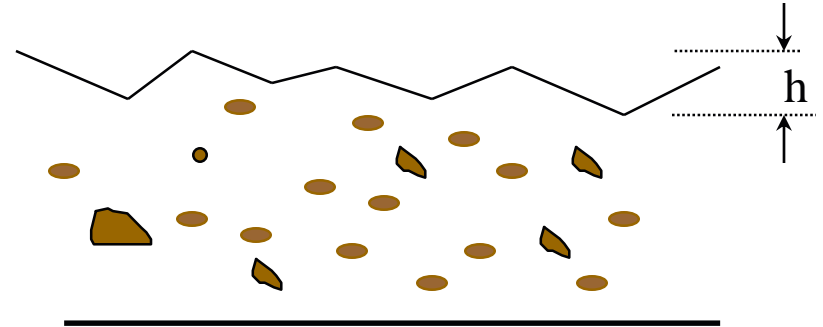
$G = \cos^2 \theta$

Coppo's model: 1.4 to 36.6 GHz,  
an angle range of 10~60 degree.

$$P(\lambda, \sigma; A) = \exp\left(-A\sqrt{\frac{\sigma}{\lambda}}\right)$$

Wegmüller model: 1 to 100 GHz, the incidence  
angles from 20 – 70 degree

$$P = \exp\left(-(k\sigma)^{\sqrt{0.1 \cos \vartheta}}\right)$$



$m_v$  - volumetric moisture

$\epsilon$  - dielectric constant of soil solids

$\rho_b$  - density of soil

$\rho_s$  - density of solids

S - sand fraction

C - clay fraction

h - roughness height

q- cross-polarization factor

# Improved Surface Roughness Model

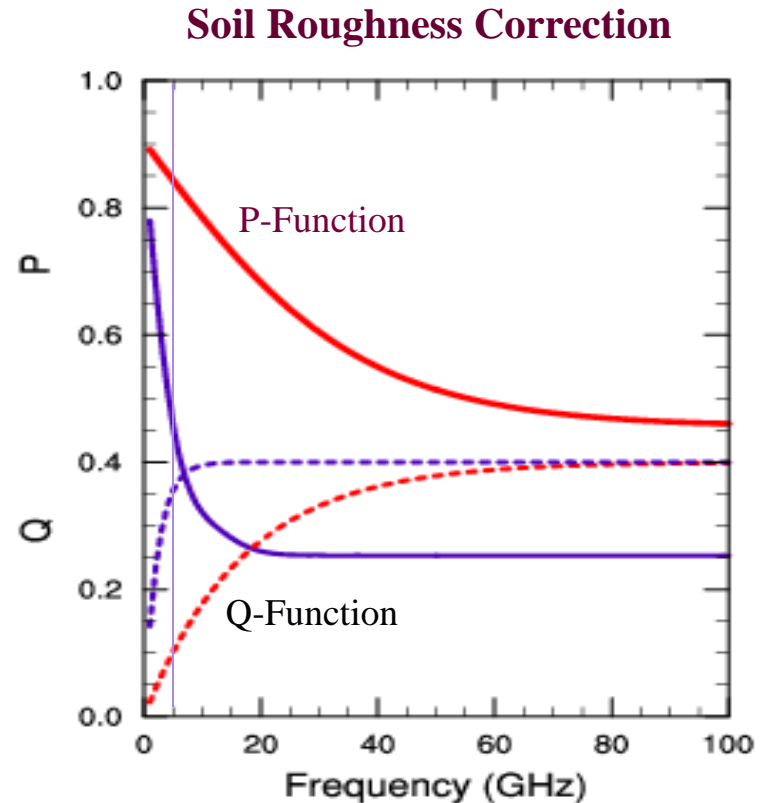
**Attenuation Function:**

$$P(k, \theta, \sigma) = \frac{1}{2} \left[ A + B \tanh\left(\frac{x - x_0}{w_0}\right) + c \tanh\left(\frac{x - x_0}{w_1}\right) \right]$$

$$x(k, \theta, \sigma) = 2k\sigma \cos(\theta) \quad k = 2\pi f / 30$$

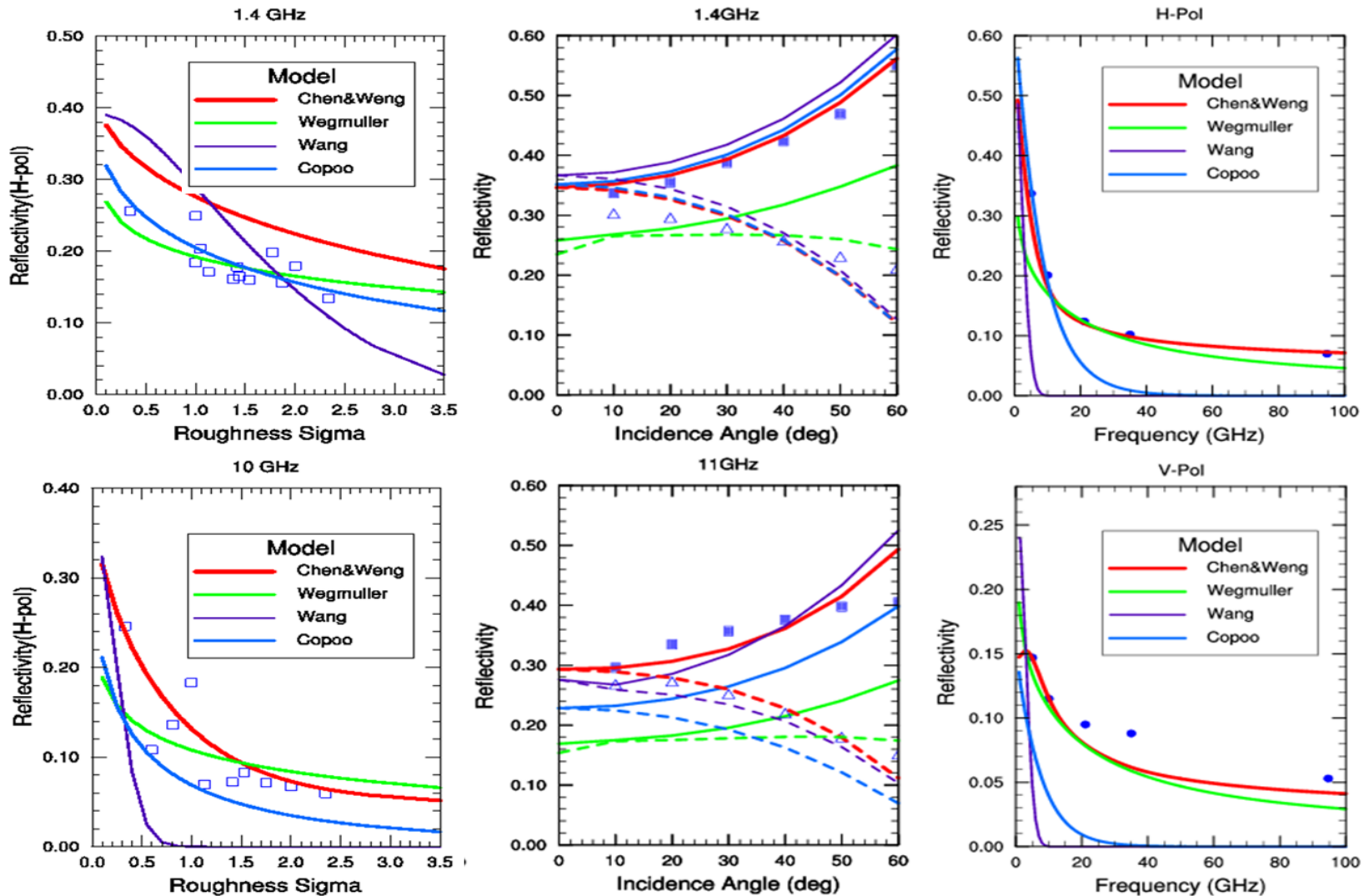
**Cross-Polarization Function:**

$$Q(\kappa, \sigma, \theta) = B_1 (1 - e^{-B_2 \kappa \sigma \cos^2 \theta})$$

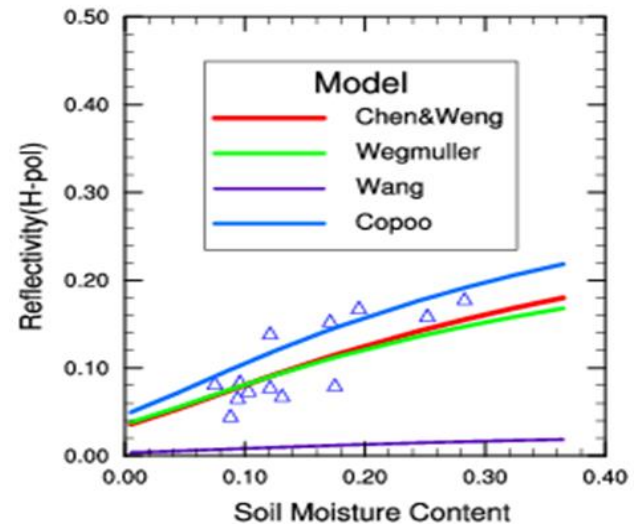
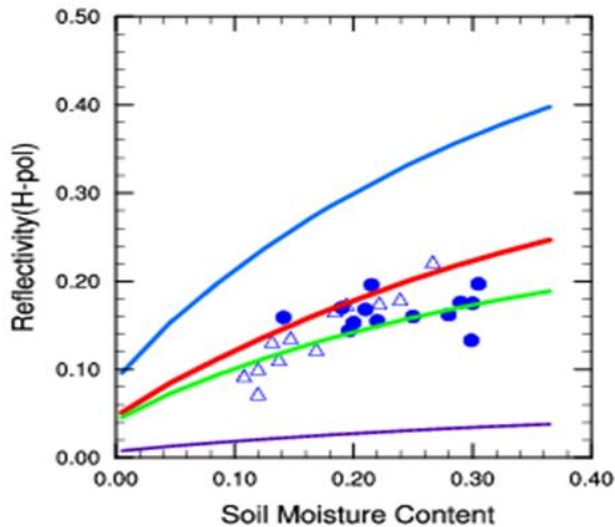
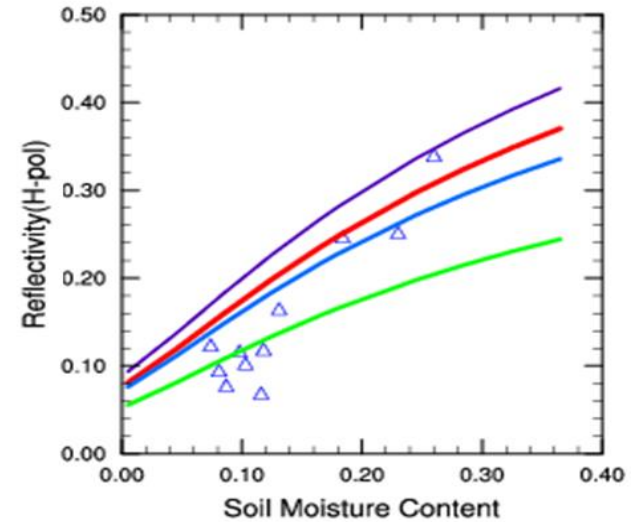
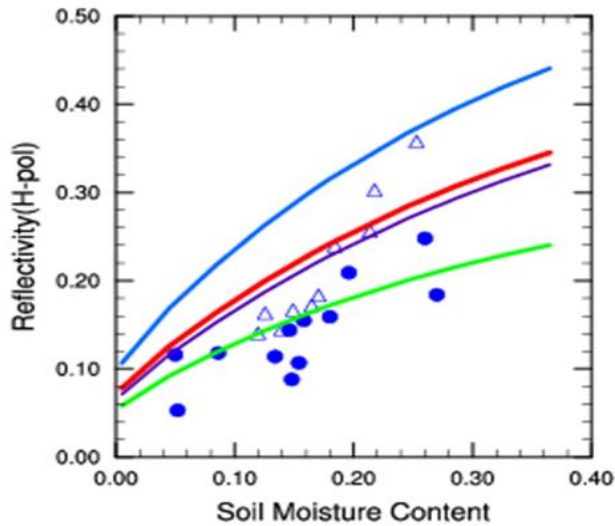




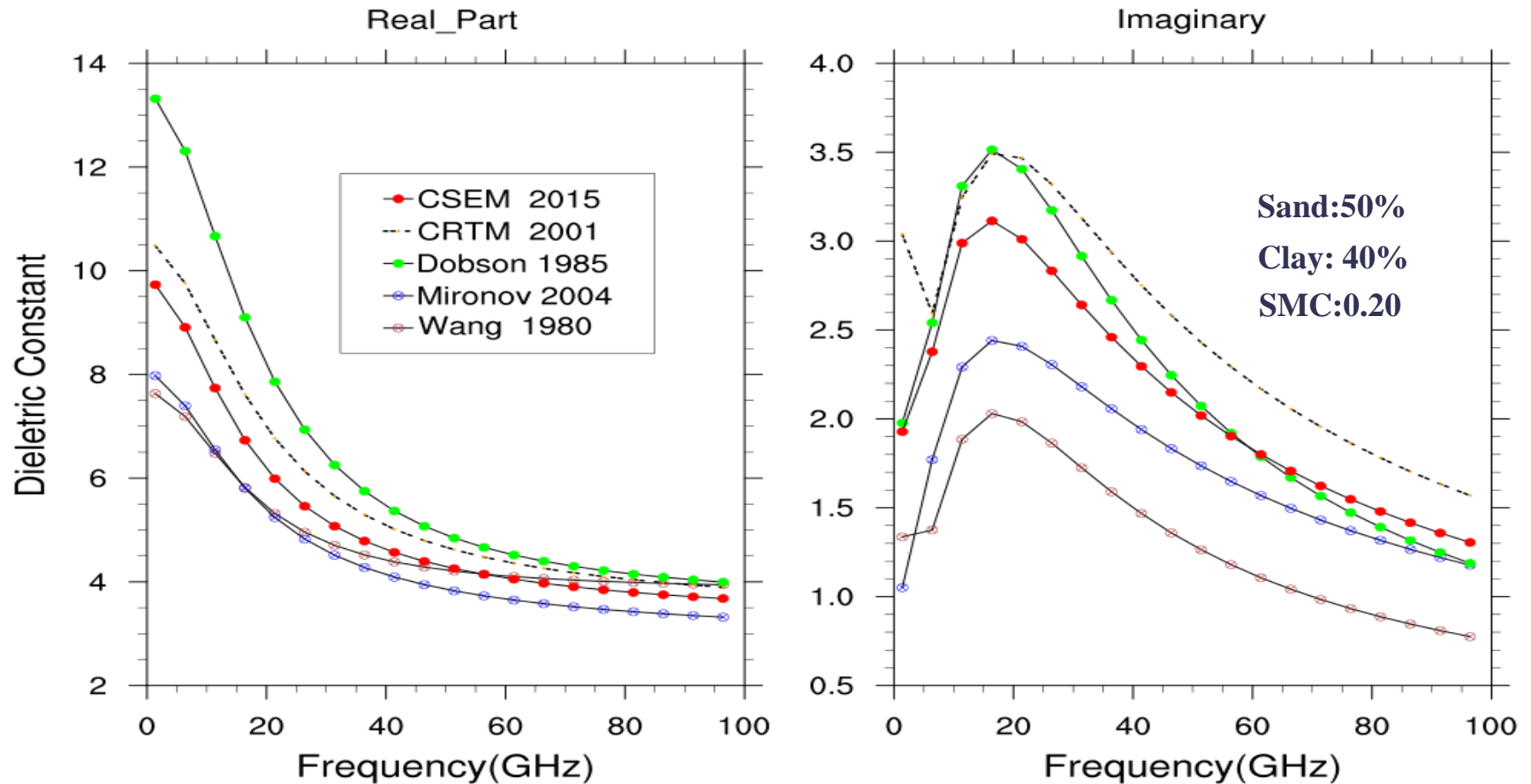
# Verification of MW Soil Emission Model with Ground Measurements (1)



# Verification of MW Soil Emission Model with Ground Measurements (2)



# Optimization of MW Soil Dielectric Model



There also exists large uncertainty in the calculation of the MW soil permittivity. Several soil MW permittivity models (Weng et al 2001; Wang et al, 1980; Mironov et al, 2004; Dobson et al., 1985 ) are implemented in CSEM for research purpose and model optimization purpose.

# Optical Properties of Dense Medium

Small perturbation method  
(Tsang et al., 1985)

$$\epsilon_{eff} = \frac{1 + 2f_a y}{1 - f_a y} + i \frac{2f_a y^2 (ka)^3 (1 - f_a)^4}{(1 - f_a y)^2 (1 + 2f_a)^2}$$

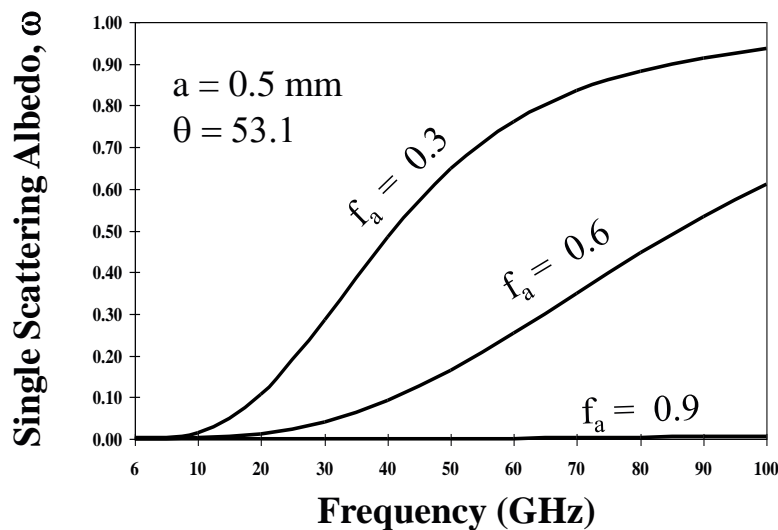
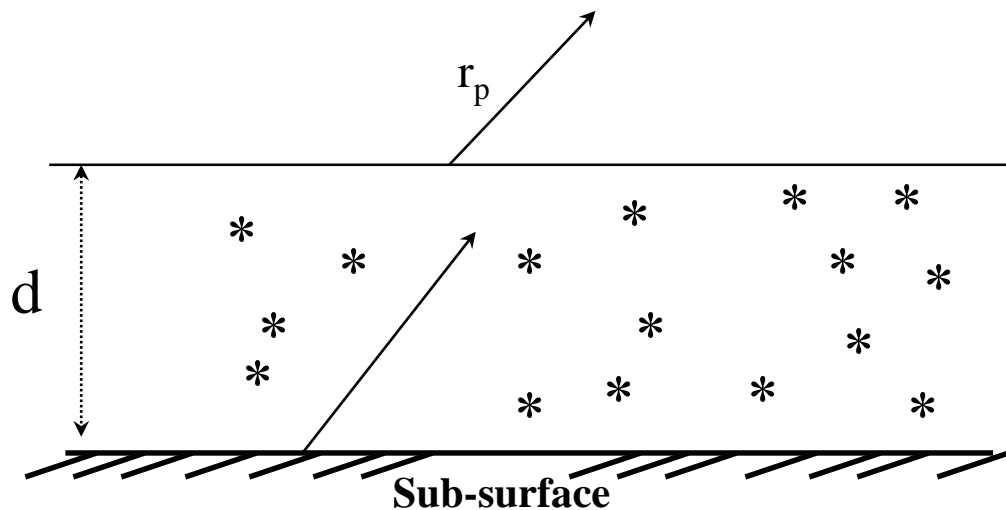
$$\kappa = \sqrt{3(1 - \omega)(1 - \omega g)}$$

$$y = \frac{\epsilon_s - \epsilon}{\epsilon_s + 2\epsilon}$$

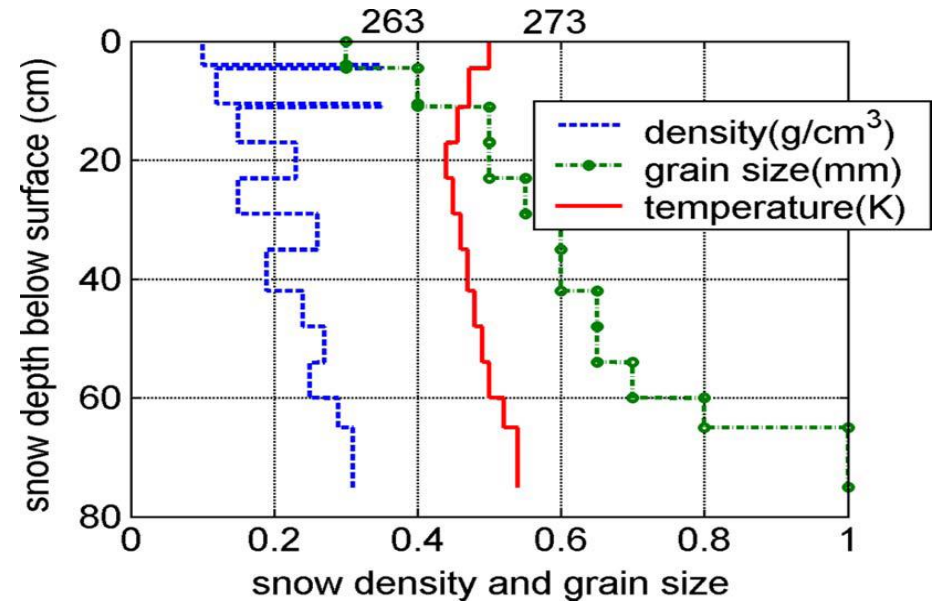
$f_a$  - ice-volume fraction

$d$  - snow depth

$a$  - snow particle size



# Multilayer Snow Emissivity Modeling



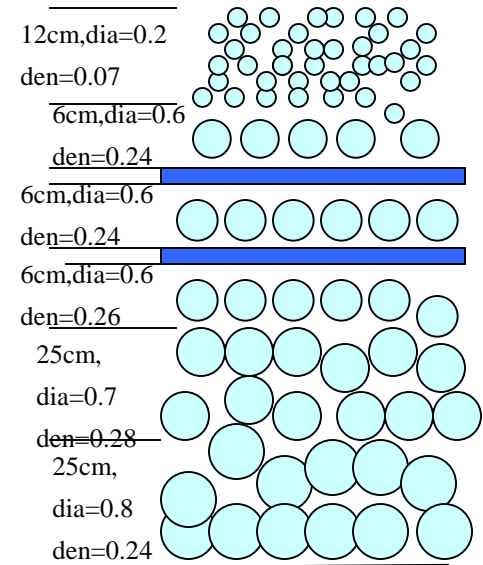
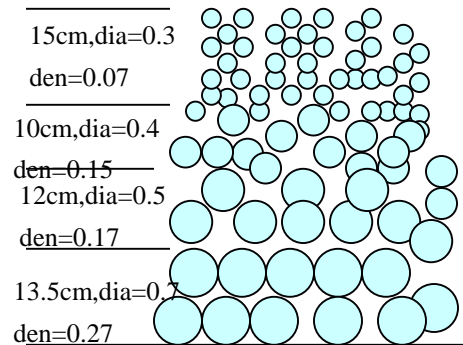
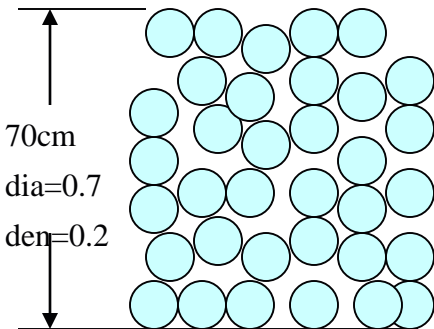
Input snow parameters: **grain size profile, density profile, temperature profile**

# Conceptual Model for Vertical Stratification

1. New snow pack vertically homogeneous layer

2. New snow with small grain size accumulated on thick snow pack

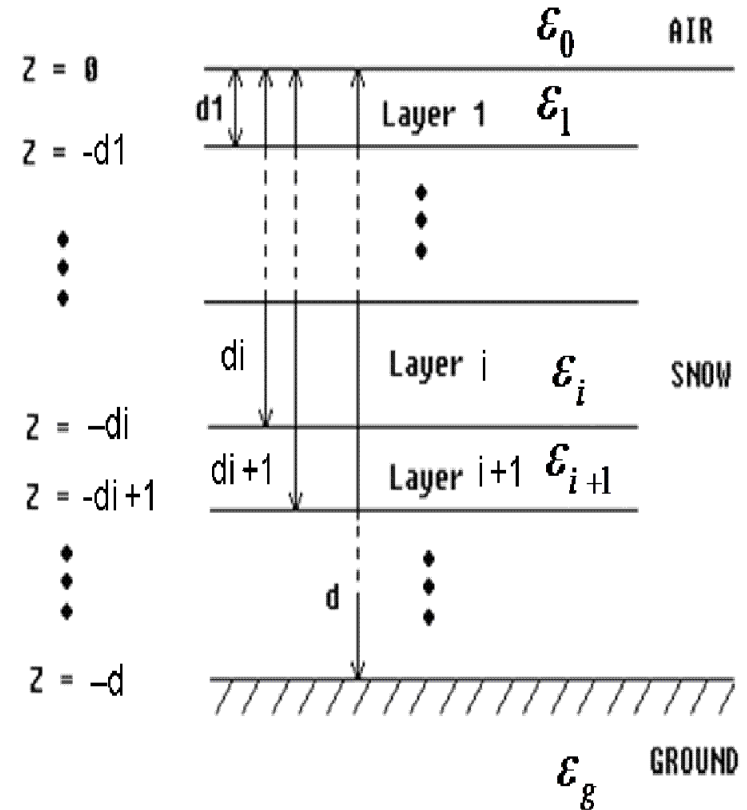
3. New snow with small grain size accumulated on thick snow pack with ice crusts



# Dense Media Radiative Transfer Equation

**Dense media radiative transfer (DMRT) equations in layer  $i$**  (Liang and Tsang, 2009) :

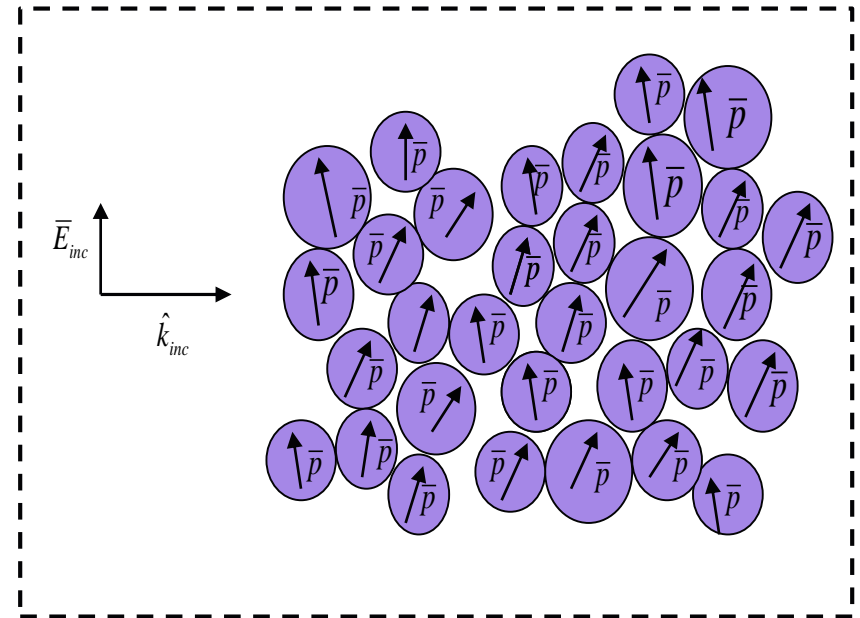
$$\cos \theta \frac{d\bar{I}_i(\theta, z)}{dz} = -\kappa_{ei} \cdot \bar{I}_i(\theta, z) + \kappa_{ai} T^i + \int_0^\pi d\theta' \sin \theta' \bar{P}_i(\theta; \theta') \bar{I}_i(\theta', z)$$



where phase matrix and extinction coefficients are computed using QCA

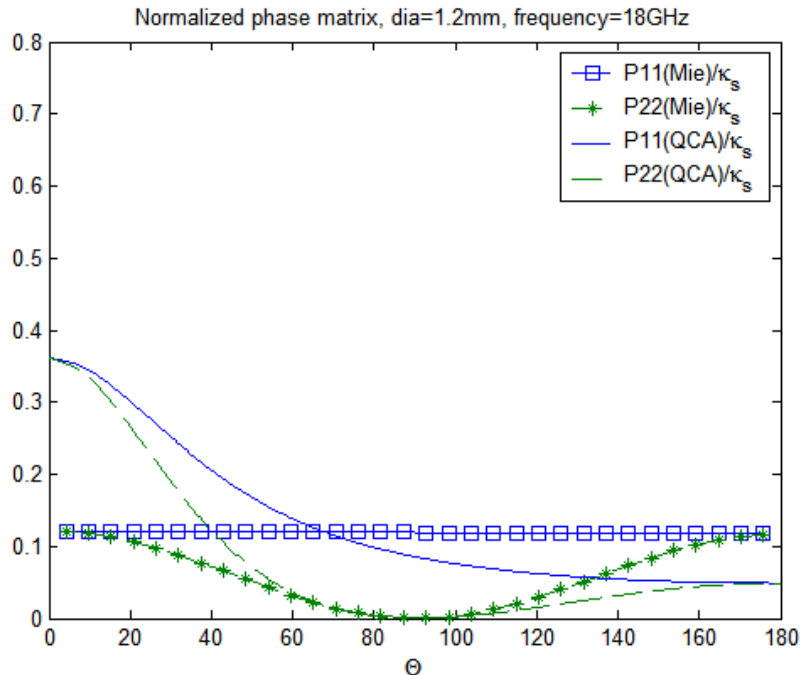
# Dense Media Including Collective Scattering Effects

- Snow , dense media ; Particles lie in close proximity much closer than a wavelength; many particles in one wavelength tube
- Induced dipoles in the particles affect each other, near field coherent interactions
- Mutual coherent wave interaction depends on particles' relative positions, i.e. pair distribution functions





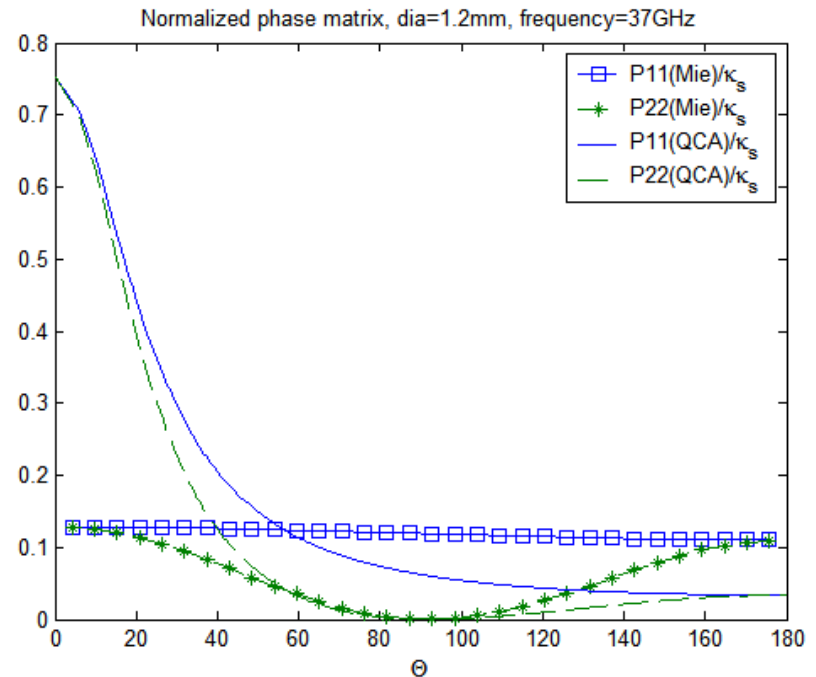
# Phase Matrix: QCA compared with Mie Theory



$a = 0.06\text{cm}$

$f = 0.2$

frequency = 18GHz,



$a = 0.06\text{cm}$

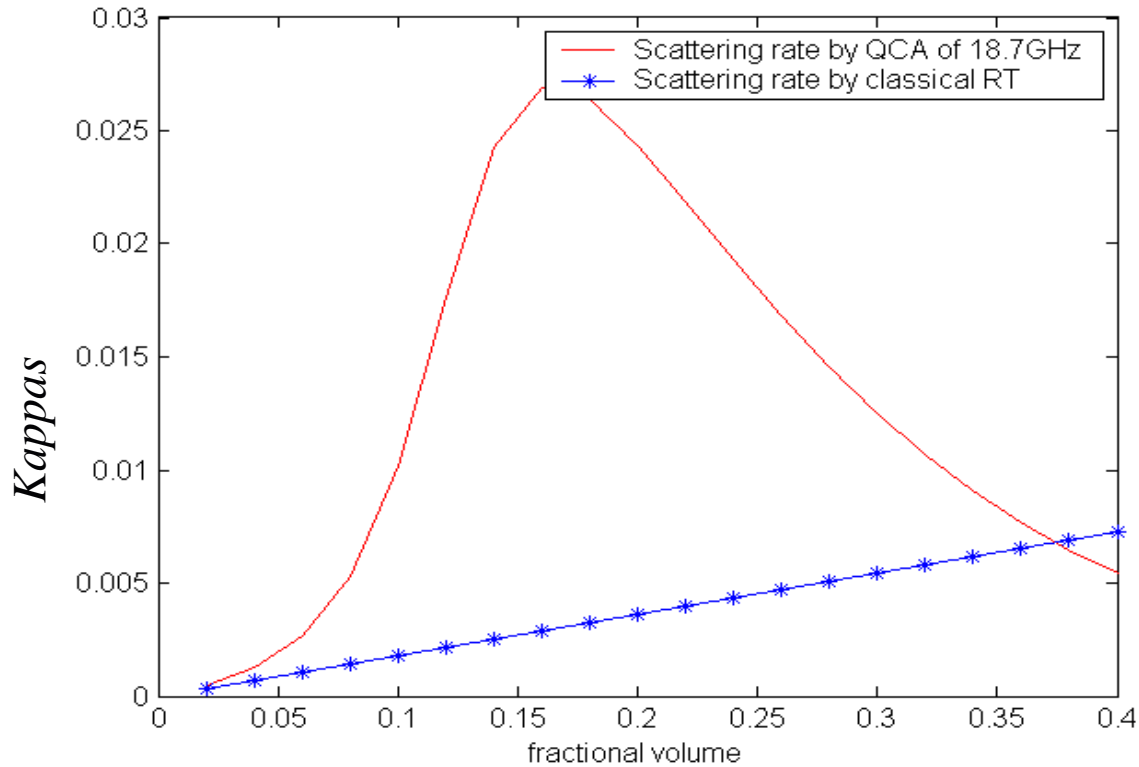
$f = 0.2$

frequency = 37GHz,

*Sticky particles (QCA) have larger forward scattering*

*Sticky particles (QCA) tends to form cluster to have larger effective size*

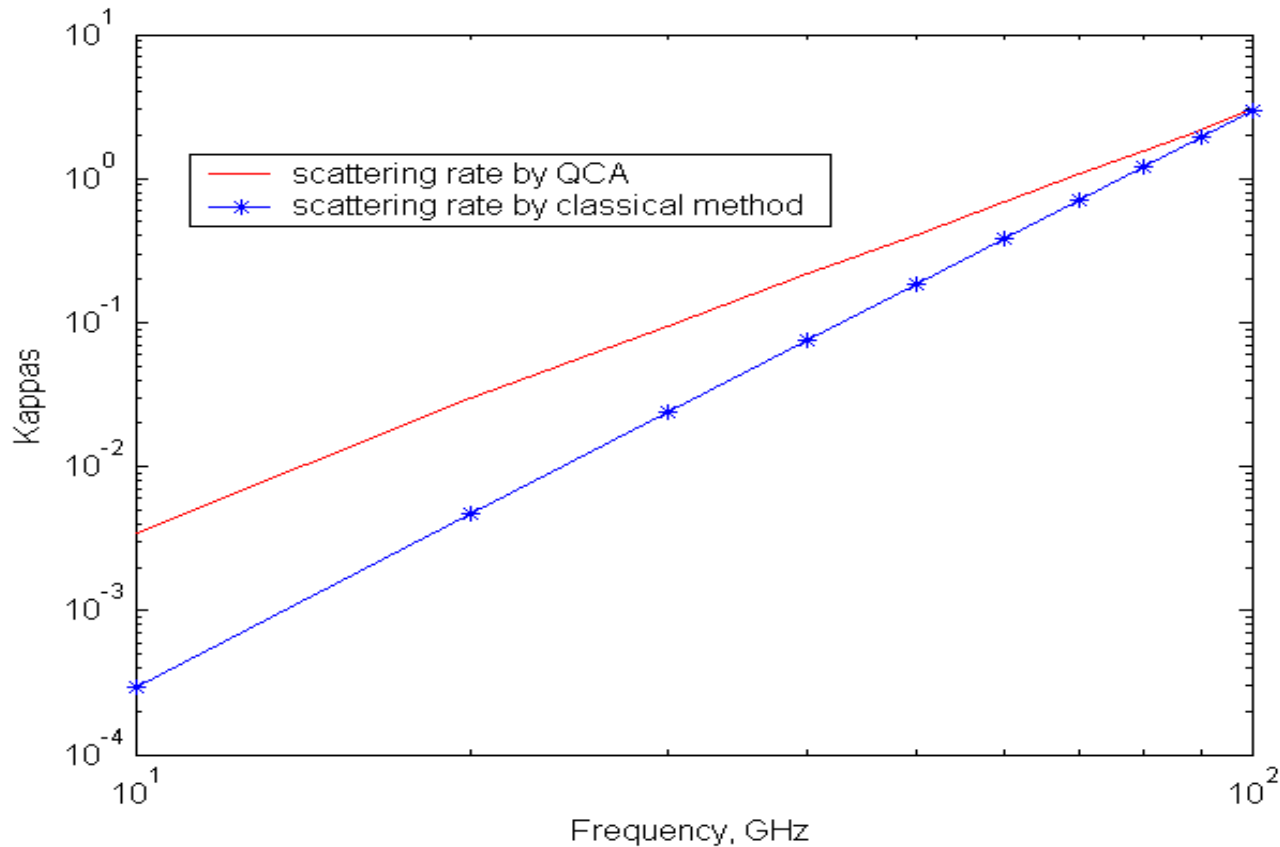
# Scattering Efficiency vs Fractional Volume



$a=0.06\text{cm},$   
 $frequency=18.7\text{GHz}$

*Kappas of QCA is nonlinear of fractional volume in dense media scattering*

# Scattering Rate: QCA Compared with Mie Theory

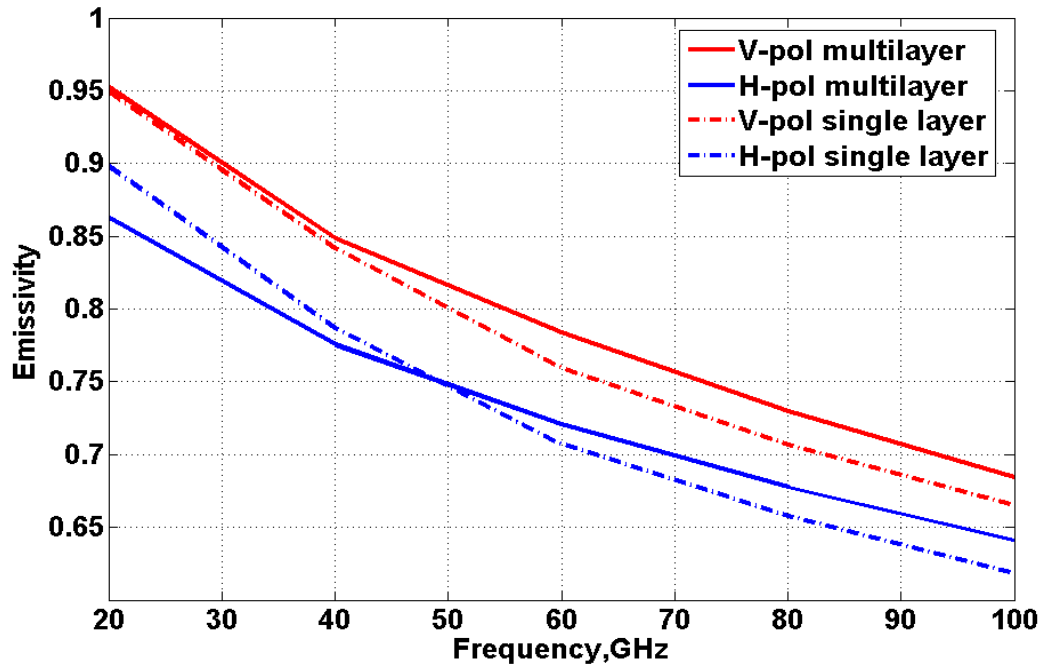


Diameter:  $2a = 0.12\text{cm}$

fractional volume:  $f=0.2$

QCA has weaker frequency dependence

# Multilayer vs Single Layer Model Results

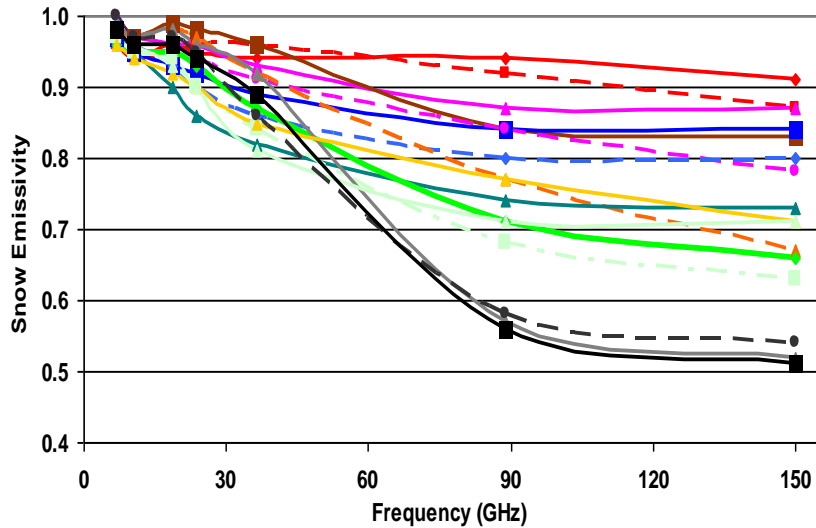


Multi-layer model predicts **larger polarization difference** and **lower frequency difference** than a single-layer snow model

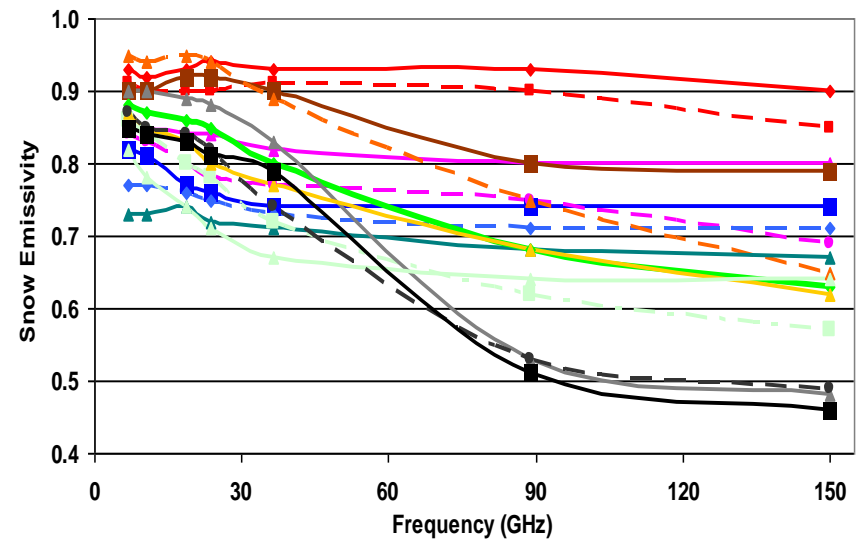
Multi-layer model predicts **higher emissivity** than a single-layer snow model at high frequency

# Snow Microwave Emissivity Spectra

Snow V-POL Emissivity Spectra



Snow H-POL Emissivity Spectra

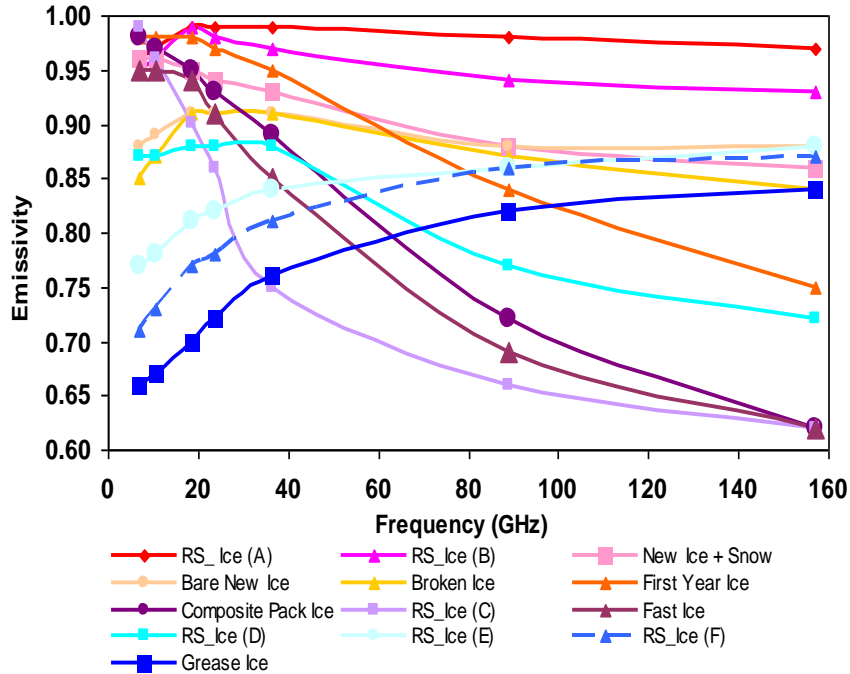


- Grass\_after\_Snow
- Shallow Snow
- Thin Crust Snow
- Bottom Crust Snow (B)
- RS\_Snow (B)
- RS\_Snow (E)
- Wet Snow
- Medium Snow
- Thick Crust Snow
- Crust Snow
- RS\_Snow (C)
- Powder Snow
- Deep Snow
- Bottom Crust Snow (A)
- RS\_Snow (A)
- RS\_Snow (D)

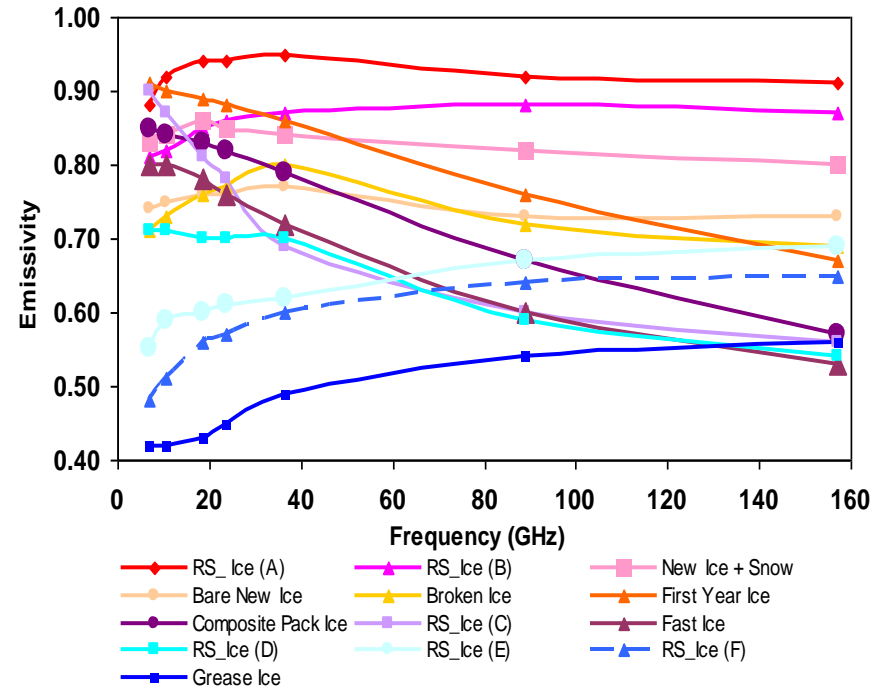
- Grass\_after\_Snow
- Shallow Snow
- Thin Crust Snow
- Bottom Crust Snow (B)
- RS\_Snow (B)
- RS\_Snow (E)
- Wet Snow
- Medium Snow
- Thick Crust Snow
- Crust Snow
- RS\_Snow (C)
- Powder Snow
- Deep Snow
- Bottom Crust Snow (A)
- RS\_Snow (A)
- RS\_Snow (D)

# Sea Ice Microwave Emissivity Spectra

Sea Ice V-POL Emissivity Spectra

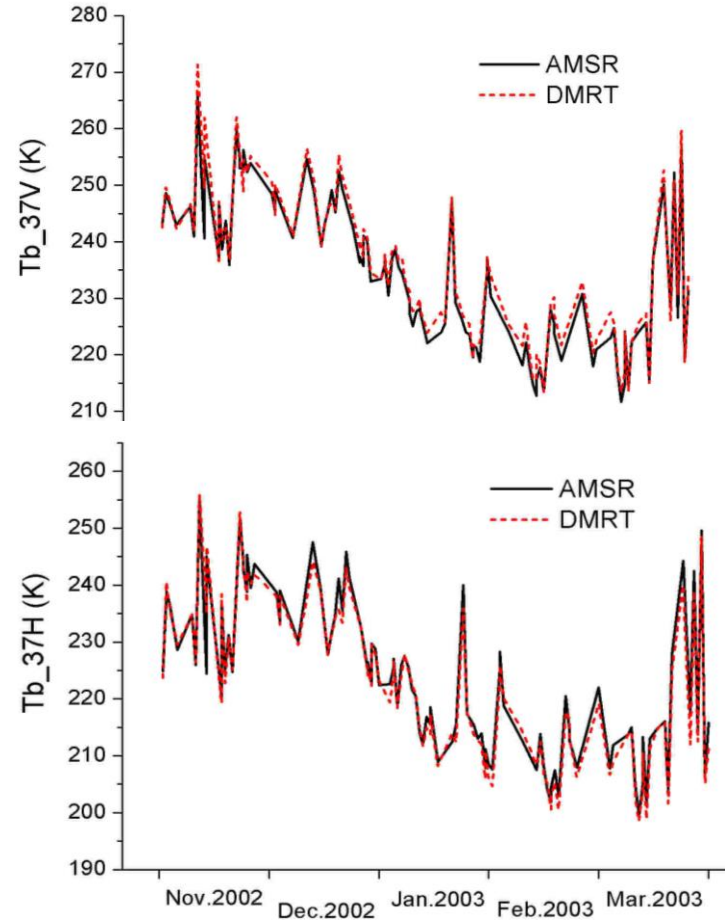
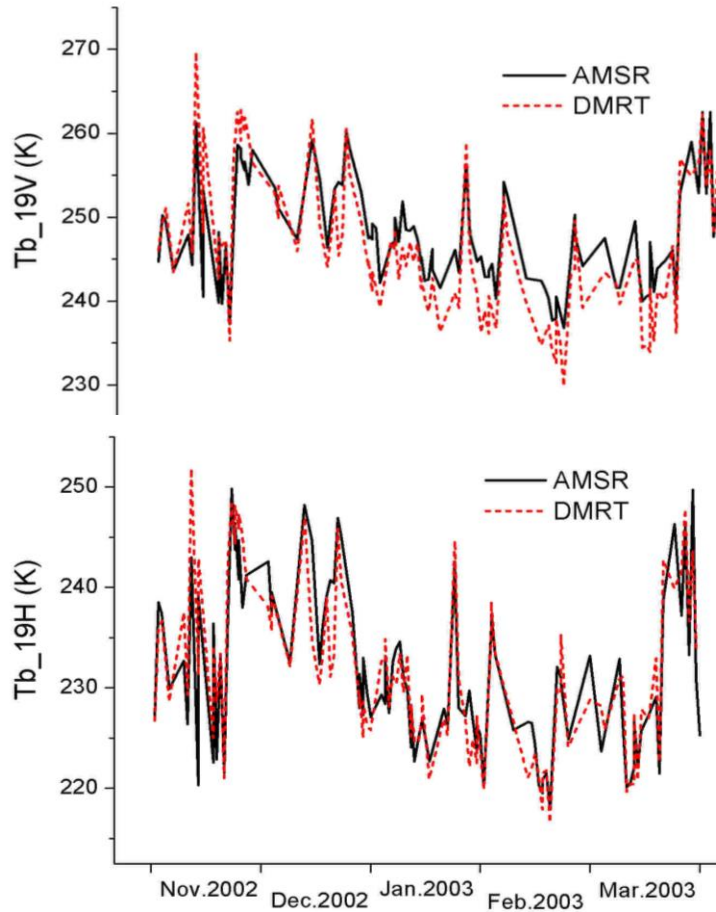


Sea Ice H-POL Emissivity Spectra

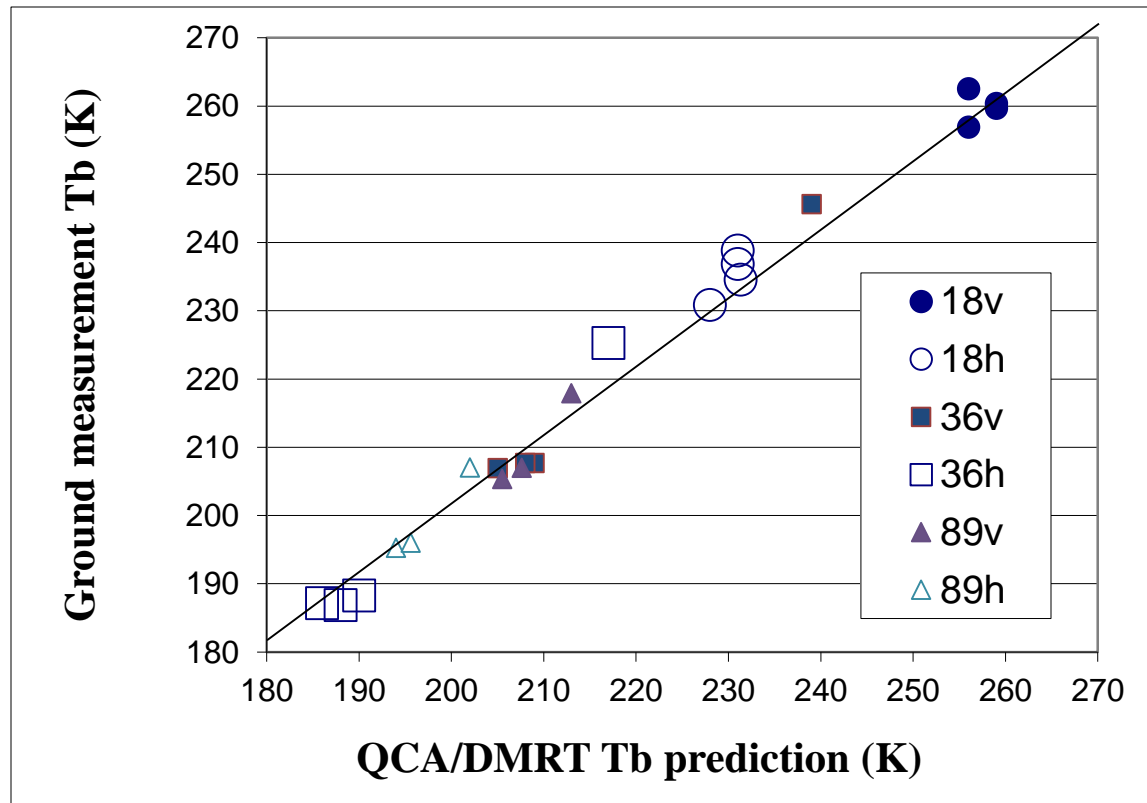


# Comparison of DMRT with AMSR Measurements

WMO 71825, 52N, 66W, 2002, 11, 1~2003, 3, 31



# Validation of QCA/DMRT Brightness Temperatures with GBMR Observations

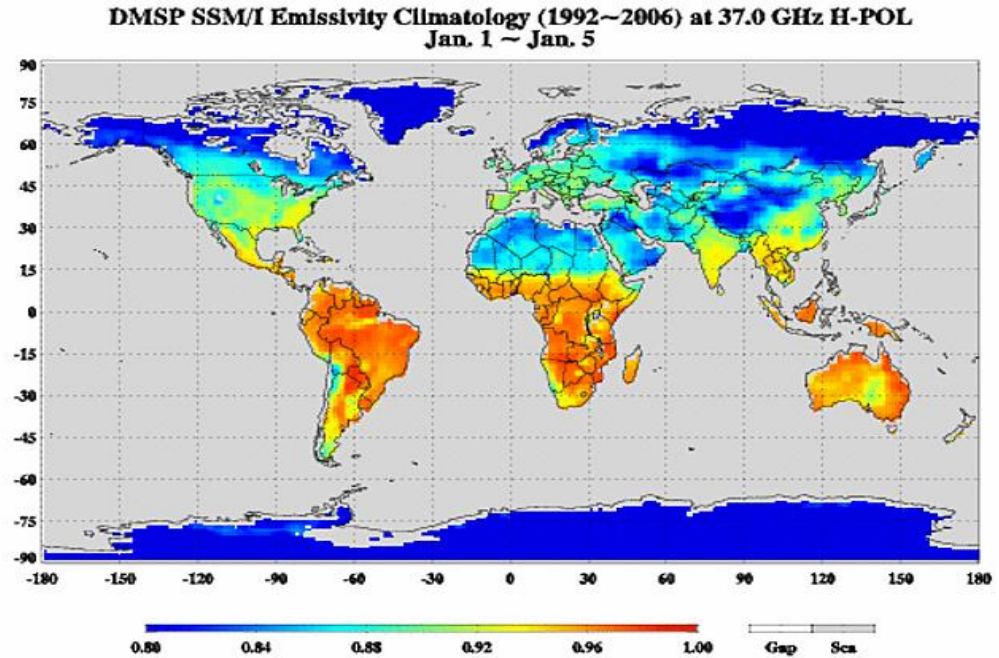


**The model Tb prediction shows close agreement with the ground Tb observation**



# Global Land Emissivity Characterization SSM/I Fifteen Year Time Series

- Large season change at higher frequencies
- Large polarization difference for several surfaces (e.g. desert, snow, flooding)
- Deserts appear as a scattering medium



*Click following hyperlinks for other channel emissivity pentad looping images*

19V

19H

37V

37H

85V

85H

*SSM/I surface emissivity climatological data set is developed at various time scales (e.g. pentad, weekly and monthly, anomaly). SSM/I sensors from F10 to 15 satellites are intercalibrated to a reference satellite (F13)*

# Summary and Conclusions

- Developed physical modules for surface optical properties
- Improved the surface roughness models (e.g. two-scale model of oceans and Rayleigh approximation of land roughness height)
- Radiative transfer solvers for surface media could be very complex and require considerations of coherent scattering when the particles are close to each other (e.g. surface snow)
- Full polarimetric Stokes components should be included when two media forms a clear interface (e.g. air/snow, air/water)
- Surface scattering related to snow grain, leaf and quartz must be derived through generalized scattering theory (e.g. discrete dipole approximation)
- The permittivity for some soil types at certain wavelength is largely unknown and can be inferred if the spectral properties in other regions are measured
- Remote sensing of surface emissivity is also an active topic and requires removal of atmospheric contributions to the satellite radiances and also a good quality control for removing cloud effects